THE UNIVERSITY OF ALBERTA

INTERACTION OF CONCRETE MASONRY BEARING WALLS AND CONCRETE FLOOR SLABS

by

STUART NEIL FERGUSON

A THESIS

SUBMITTED TO THE FACULTY OF GRADUATE STUDIES AND RESEARCH

IN PARTIAL FULFILMENT OF THE REQUIREMENTS FOR THE DEGREE

OF MASTER OF SCIENCE

DEPARTMENT OF CIVIL ENGINEERING

EDMONTON, ALBERTA

SPRING 1979

Abstract

Present design practice for masonry bearing walls is based on converting wall moments to equivalent eccentricities of the axial load on the wall. Few guidelines are given for the determination of moments transferred to the walls from a loaded floor slab. The purpose of this study is to examine the behavior of masonry wall-floor slab combinations and to analyse the relationship between axial load levels on a wall and the degree of moment resisted by the wall-slab joint.

A series of 16 masonry wall-floor slab combinations were tested in the I.F. Morrison Structural Engineering Laboratory at the University of Alberta under the supervision of Dr. J. Warwaruk. The major variables were: the level of axial load on the wall, the amount of vertical reinforcement in the wall, and the type of joint detail provided at the wall-slab connection.

Acknowledgement

The author wishes to express his appreciation to the following persons and organizations for their various contributions to this thesis:

Professors J. Warwaruk and J. Longworth for their enthusiasm and expert guidance;

The University of Alberta for the use of the I.F. Morrison Structural Laboratory and the Textform facilities for reproducing this thesis;

Edcon Block and Con-force Products Co. for their donations of materials used for these tests;

The Alberta Masonry Institute and the National Research Council for their generous financing of the testing program;

The National Research Council for personal financial assistance in the form of a graduate scholarship;

Mr. Larry Burden and the technicians at the I.F. Morrison Lab. for their experience, patience and energy which allowed the testing program to be completed smoothly.

Table of Contents

List of Tables

List of Figures

List of Plates

Notation

Dimensions and Section Properties

As = area of reinforcing steel

Asc = area of compression reinforcement

BB = width of section under consideration

c = depth to neutral axis

e = eccentricity

h = height of wall

I = moment of inertia

Ie = effective moment of inertia of a cracked wall about the centroid

Ieu = effective moment of inertia of the upper wall

Icr =cracked moment of inertia of a cross section

Iel = effective moment of inertia of the lower wall

t = thickness of the cross section

Material Properties

E = modulus of elasticity

Ec = modulus of elasticity of concrete

Em = modulus of elasticity of masonry

Es = modulus of elasticity of steel

Forces and Moments

M = moment

Ml = moment on lower wall

Mu = moment on upper wall

Mmax = maximum applied moment

Mpl = moment at which joint begins to rotate plastically

Msl = applied moment from slab

Mult = ultimate moment

P = applied load

Pb = applied load at balanced failure

Pcr = critical or buckling load

P-Delta = moment caused by axial load and deflection of the wall

Stresses and Strains

f'c = ultimate compressive strength of concrete

f'm = ultimate compressive strength of masonry

fy = yield stress of reinforcing steel

sigma1 = maximum stress at outer fibre

sigma2 = minimum stress at outer fibre

Miscellaneous

w/c = water to cement ratio

θh = measured rotation of a horizontal member

$\theta hdef$ = rotation of a horizontal member computed from the deflected shape

θv = measured rotation of a vertical member

θvl = rotation of the upper wall end

θvu = rotation of the lower wall end

ϕ = difference between the rotation of a horizontal member and a vertical member

ϕult = ultimate plastic joint rotation

1. INTRODUCTION

1.1 Background Information

Masonry construction in its basic form is one of the oldest types of construction known to man. From the massive pyramids of Egypt, the Roman Arch, and on to the hugh domed and buttressed cathedrals of Europe; masonry has evolved into the modern sophisticated high-rise construction of today.

With the advent of high strength concrete blocks in North America 15 to 20 storey masonry bearing wall buildings can be found in most cities. Economic and architectural aspects of masonry have allowed it to compete with reinforced concrete and steel in high-rise projects, and in the future even taller structures may be built.

As the buildings become taller the design of the bearing wall becomes more sophisticated. Economy rules that massive walls can not be relied upon to carry the loads of such tall structures. Whereas masonry was once used only for its compressive strength it must now be designed for flexural stresses resulting from moments transferred from floor slabs resting on or being clamped between the walls.

This intricate type of design requires that the designer must have a clear understanding of the behavior of the structure and the materials used to build it. Present design practice dictates that the designer must rely on his own judgement in assessing the interaction of the structure

and with his lack of understanding of masonry the designer tends to choose the more researched materials such as reinforced concrete and steel.

The need for research on masonry is clearly known. The behavior of masonry walls under combined axial load and moment has been studied extensively by various authors. A research program at the Univerisity of Alberta has examined the load carrying capacity of plain and reinforced masonry walls. However, the interaction of the wall-slab connection has not been examined greatly. While some tests have been conducted and documented by various authors, the results of these tests are inconclusive and the empirical relationships are presented in a form much too complex for the designer to use.

While this study is not conclusive in itself, it is expected that the theoretical findings and experimental data presented here will add to current research and point the way to further research eventually leading to design rules as complete and simple to use as those for reinforced concrete and steel.

1.2 Object and Scope

The main objectives of this study are:

a. To examine existing theories for evaluating wall-joint-slab performance.

b. To observe behavior, cracking and failure types of various wall-slab combinations.

c. To examine the relationship between axial load and joint performance of wall-slab combinations as it relates to moment resistance.

d. To determine if masonry wall-floor slab interaction can be analysed by existing rigid frame analysis procedures.

e. To lay foundations for further study of related masonry aspects.

2. REVIEW OF PREVIOUS WORK AND PRESENT DESIGN PRACTICE

2.1 Introduction

A brief review of the previous research and present design practice is presented in this chapter.

Eccentricity of load on a load bearing masonry wall may result from moments transferred to the wall from a loaded floor slab. This type of equivalent eccentricity, of prime importance in the determination of wall capacity, is subject to considerable discussion by engineers. Limited investigation has been carried out by researchers on wall-floor slab interaction and some progress has been made in understanding and predicting the performance of the wall-floor slab joint. More recent research is leading to a better evaluation of masonry wall performance and the development of new design methods for load bearing masonry walls.

At the present time, load bearing masonry wall design in North America is based on a working stress approach. Moments on a wall are converted to equivalent eccentricities of the axial load. Slenderness of walls and eccentricity of load are evaluated with the use of empirical coefficients which reduce the allowable axial load on a wall depending on the magnitude of the wall slenderness and eccentricity of axial load. Few guidelines are available for the determination of the eccentricity of load. Hence the magnitude of the eccentricity is based on the judgement of

the individual designer.

2.2 Review of Previous Work

2.2.1 Wall/Floor Slab Behavior

Research on masonry wall-floor slab interaction has been limited and scattered. However a few researchers have conducted tests over the past 20 years. While the information obtained has allowed some understanding on the phenomena of joint failure it is too inconclusive to employ as a basis for a design procedure.

The first documented tests on joint behavior were performed by Sahlin[1] in 1959 when he began testing frame structures of brick masonry walls and concrete floor slabs. First Sahlin related the compression load on a wall to its vertical position in the building. The eccentricity of the load on the wall was then obtained by dividing the negative moment on the slab end by the axial load on the wall. The problem which Sahlin attempted to solve was to determine the amount of negative moment in the slab end or conversely the amount of fixity provided by the clamping action of the wall and by the stiffness or resistance to rotation of the wall.

In a more recent paper Sahlin[2] stated that "A fundamental point in the theory of interaction of walls and slabs is the joint behavior". He then related the behavior in terms of rotations of the wall, the slab and the joint.

$$\theta h = \theta v + \emptyset$$

Where θh is the amount of rotation of a horizontal member,

θv is the amount of rotation of a vertical member and $\emptyset$ is the difference between the rotation of a horizontal member and a vertical member.

There are three possible failure modes for the frame:

a. The joint remains rigid ($\emptyset = 0.$) and the wall fails due to buckling or due to eccentric loading two or three bricks below the slab. In this case the negative moment at the slab end can be evaluated by various means taking into consideration frame action and reduced stiffness of the wall due to cracking.

b. The joint becomes "plastified" ($\emptyset > 0.$). Above a certain moment, Mpl, the joint begins to rotate with the moment remaining constant or decreasing. If the slab is stiff enough to prevent large end rotations, the joint remains intact and failure occurs when the load reaches the ultimate capacity of the wall. In this case the negative moment at the slab end would be Mpl and P and e could easily be determined. Since the moment remains constant, increasing the slab load and thus the compressive load on the wall results in a reduced eccentricity.

c. If the joint becomes "plastified" and the slab is flexible enough to permit further end rotations, the joint could fail by reaching its ultimate rotation capacity ($\emptyset = \emptyset ult$). The failure is then localized at the joint and crushing of the blocks immediately

above and below the joint results. Sahlin states that this type of failure is principally separated from the failure of the wall. However, the rotation capacity of the joint is governed by the axial load on the wall. As the axial load on the wall increases the ultimate rotation capacity of the joint decreases.

In all of the above cases it was assumed that the negative moment capacity of the slab is not exceeded. If it were, the moment transferred to the wall would be equal to the negative moment capacity of the slab.

Sahlin[3] provided a theoretical explanation of the interaction and developed equations for the calculation of wall, slab and joint rotations. The equations are extremely complex and basic assumptions must be made regarding Mpl and Øult before they can be used. Before calculations can be made to determine the failure mode and the failure load for a wall-slab combination, the values of Mpl and Øult must be determined experimentally for the specific material, joint detail and loading condition.

Sahlin[2] suggested that in further tests more attention should be paid to the angle of rotation of the wall ends than mid-height deflections usually determined and reported in tests on masonry walls.

The effect of mortar strength on the joint rotation of brick wall-floor slab joints was investigated by Maurenbrecher and Hendry[4]. They concluded that while

initially all specimens performed similarly, the walls with lower strength mortar allowed more rotation of the floor slab for a given slab moment. This would indicate that Mpl decreases as the mortar strength decreases, because most of the rotation occurs in the mortar joint and the lower strength mortar is more easily crushed. They also compared the effects of precompression of the walls on the degree of fixity of the joint and discovered that as the walls became more precompressed less ultimate rotation of the slab end occurred, resulting in larger moments in the walls. Walls with low precompression allowed the joint to rotate separately from the wall and failure resulted from the slab prying apart the walls and cracking the joint. They found that in a plot of moment versus joint rotation the initial slope of the graph is independent of the amount of precompressive load. Another conclusion was that as long as the joint remains elastic the level of precompression has little effect on the degree of fixity.

Further tests by Colville and Hendry[5] on two storey single bay load bearing brick masonry structures also indicated that increasing wall precompression increased joint rigidity. By analyzing rotations and deflections, they concluded that up to 75% of full fixity can be developed. Other conclusions from their tests were that the rigidity of the joint is not linearly related to increases in wall precompressions and at high precompressions the magnitude of the floor loading does not have a significant

effect on the degree of fixity.

The interaction of wall-floor slabs has been considered by many ivestigators conducting tests on the bearing capacity of masonry walls. Risager[6] considered that the angle of rotation of the slab and wall had no influence on determining the bearing capacity of the wall and is a problem which can be investigated separately. While this may be basically true, the performance of the wall-slab joint determines the amount of eccentricity of the load and the deflected shape of the wall. Sinha and Hendry[7] found that equivalent eccentricities calculated from results of their tests were less than theoretical values due to partial fixity of the joints and non-uniformity of strains.

Furler and Thurliman[8] conducted tests in which they loaded a wall axially and then applied end rotations. They discovered that as the axial load increased, the wall failed with lower end rotations. The axial load end rotation plot of their test results, with a .5mm crack width as failure criteria, looked similar to the load moment interaction curve of concrete columns and walls.

In an attempt to model the behavior of wall-slab joints Germanio and Macchi[9] tested ceramic block-concrete slab frames. They suggested that a joint could be evaluated as a partial hinge transferring a limited moment to the wall. This idealization of the joint depends on the amount of axial load on the wall. It is practical to assume that the joints act as hinges in the lesser loaded upper floors of

the building (in fact it may be best to create a real hinge to avoid cracking). In heavily loaded walls, joints behave rigidly even in the ultimate condition. Germanio and Macchi did not suggest a means of evaluating the partial moment for a case between the two extremes.

2.2.2 Wall Behavior

The behavior of eccentrically loaded walls is of prime importance when considering joint behavior of frames. Regardless of whether the joint behaves elastically or as a partial hinge, the degree of moment transferred to the wall is a function of the stiffness of both the walls and the floor slabs. Although the walls and slabs can be designed separately, their interaction is fundamental to the frame analysis of a structure.

Considerable research has been conducted during the past 20 years to evaluate the behavior of masonry walls under concentric and eccentric loads. The most recent research was carried out by Hatzinikolas[10] at the University of Alberta. He tested sixty-eight full scale walls under various loading conditions. A moment magnifier procedure, which accounts for wall slenderness and eccentricity of load, was used to evaluate the strength or capacity of a wall. To use the moment magnifier procedure Hatzinikolas developed a method to predict the stiffness of a cracked wall subjected to an axial load. Possibly this method could be used in frame analysis of a structure, where a value for

the stiffness of the walls and the slabs is required.

2.3 Present Design Practice

Most present day building codes for masonry construction include a design procedure for walls subjected to eccentric loading. Once the eccentricities of the loads are chosen the designer can readily determine the allowable load on a wall. However, none of the building codes recommend a method, or give guidelines, for determining the eccentricity of the load. The designer therefore must use his own judgement in computing the moment transferred from the slab to the wall.

The Structural Clay Products Institute[11] suggests that the assumption of full fixity of the joint is conservative. However they caution that in upper stories this assumption could lead to cracking of the joint, and, in lower stories local overstressing could be a problem. They also suggest that as creep deflection of the slab increases, the fixing moment decreases.

The Clay Brick Association of Canada[12], considers that the type of construction and loading sequence both play an important part in the amount of fixity in the wall-slab joint. For example, a precast slab or a cast-in-place slab with shoring removed before the upper levels are built should to be treated as simply supported for dead loads and fixed for live loads. They indicate that it is logical to assume full fixity for lower floors while it is the

designer's advantage to use a simply supported end condition for upper floors.

3. EXPERIMENTAL PROGRAM

3.1 Materials

Materials used for the construction of the test specimens were purchased locally and were representative of materials commonly used in the Edmonton area.

3.1.1 Concrete Block Units

Four basic units were used for the construction of all test specimens, namely 8x8x16 inch stretcher block, 8x8x16 inch end block, 8x8x8 inch half block and, in the case of precast slabs, 8x16x1.5 inch slab block to face the wall at the slab level. The units are shown schematically in Fig. 3.1 and the physical properties of the units are listed in Table 3.1.

3.1.2 Mortar

All specimens were constructed using Type S mortar consisting of one part normal portland cement, one-half part hydrated lime and four parts sand. The mortar was mixed by hand in approximately 1/9 cubic yard batches and water was added as directed by the mason. Twenty four 2 inch mortar cubes were made from the batches and were cured in the lab at a relative humidity of 30%. Six of the cubes were placed under wetted burlap. Of the eighteen dry cured cubes, the average 28 day strength was found to be 700 psi and the six wetted cubes had an average 28 day strength of 1860 psi.

3.1.3 Grout

A mixture of pea gravel and natural sand was used to grout the reinforced walls and the precast slab-wall joint. The mix was proportioned by weight using Type III normal portland cement. The proportions were 88 lbs cement, 345 lbs sand and 245 lbs pea gravel with a w/c ratio of 1. Thirteen 4x4x8 inch grout specimens were prepared and cured according to ASTM Standard C595-74. The average 28 day compressive strength of the grout was 1200 psi.

3.1.4 Concrete

A mixture of normal weight crushed gravel and natural sand was used for the cast-in-place slabs. The mix was proportioned by weight using Type III normal portland cement. The proportions were 257 lbs cement, 379 lbs sand and 567 lbs crushed aggregate with a w/c ratio of .44. Six standard cylinders were cast and cured with the wall-slab specimens. The average 28 day compressive strength of the concrete was 4100 psi.

3.1.5 Reinforcing Steel

#3 deformed bars were used for vertical wall reinforcement and for stirrups in the cast-in-place slabs. #4 bars were used for wrap-around bars in the precast slabs and for tying precast slabs to unreinforced walls in Series D specimens. #5 deformed bars were used for the tension reinforcement in the cast-in-place slabs. The average yield

stress of two bars tested was 55.5 ksi and an idealized stress-strain relationship is shown in Fig. 3.2.

3.2 Test Specimens

3.2.1 Prisms

Five two block one mortar joint and three five-block four mortar joint prisms were built. All of the prisms had face shell mortar bedding. The dimensions of the prisms are shown in Fig. 3.3.

3.2.2 Full Scale Wall-Slab Specimens

A total of sixteen full scale wall-slab specimens were constructed. All walls were built in running bond with face shell mortar bedding, the most common practice in the construction industry. All specimens had the same vertical measurements consisting of seven bottom courses of blocks (56") an eight inch thick concrete slab and seven top courses of blocks for a total height of 120 inches.

All walls were constructed by experienced masons and were typical of walls built with good workmanship and supervision. The 3/8 inch mortar joints on both faces were cut flush and then tooled.

All walls were grouted in two lifts and the grout was vibrated into place using a one inch diameter vibrator. Cleanouts were located at the bottom of each lift to allow removal of any mortar droppings in the cores. The bottom and top courses of all walls were fully grouted to avoid

damage during transportation and local damage from the loading channels.

The sixteen specimens were divided into five categories. The slabs for Type A and B specimens were cast-in-place concrete slabs, 8 inches thick, 39.625 inches wide and extended 46 inches from the face of the wall. The slabs were reinforced with 15-#5 deformed bars and 4-#3 stirrups. The ultimate moment capacity of the slab was computed to be 1400 kip-in.

The slabs for Types C, D and E specimens were Span-Deck precast slabs, supplied by Con-Force Products Ltd., 8 inches thick, 47.625 inches wide and extended 45 inches from the face of the wall. The slabs were prestressed with four 1/2 inch 7 wire strands and were inverted so that the strands were at the top of the slab. The ultimate moment capacity of the precast slab was computed to be 835 kip-in. Because of insufficient development length for the strands, this moment may not be reached.

3.2.2.1 Type A Specimens

The four Type A specimens consisted of two wall segments 39.625 inches wide with no vertical reinforcement and 8 inch cast-in-place concrete slabs were supported at the mid-height of the specimens.

The construction sequence was as follows:

a. The bottom seven courses of the walls were laid

b. Slab forms were placed and the slabs were cast. The

slabs were cured under polyethelyne sheets for seven days after which the forms were removed.

c. The final seven courses of the walls were laid.

3.2.2.2 Type B Specimens

The four Type B specimens consisted of wall segments 39.625 inches wide, reinforced with 3-#3 bars and 8 inch cast-in-place concrete slabs were supported at the mid-height of the specimens. The construction sequence was as follows:

a. The bottom seven courses of the walls were laid.

b. The vertical reinforcement was placed and grout was vibrated into the reinforced cores to the top.

c. Slab forms were placed and the slabs were cast. The concrete was allowed to flow into the top course of the ungrouted cores. The slabs were cured under polyethelyne sheets for seven days after which the forms were removed.

d. The final seven courses of the walls were laid.

e. The vertical reinforcement for the top walls was placed and the cores grouted. A lap splice of 12 inches was provided above the slab to provide continuity of the vertical reinforcement.

Joint details for Types A and B specimens are shown in Fig. 3.4.

3.2.2.3 Type C Specimens

The two Type C specimens consisted of unreinforced wall

segments 47.625 inches wide and precast slabs supported at the mid-height. No vertical steel or wrap-around bars were placed in these specimens.

The construction sequence was as follows:

a. The bottom seven courses of the walls were laid.

b. The precast slabs were placed on the walls and the slab blocks were laid. One more course of blocks was laid above the slabs.

c. Grout was vibrated into the slabs and the courses of blocks adjacent to the slabs. Stryrofoam had been placed in the wall cores and in the slab cores to contain the grout.

d. The final six courses of blocks were laid.

3.2.2.4 Type D Specimens

The two Type D specimens consisted of unreinforced wall segments 47.625 inches wide and precast slabs at their mid-height. These specimens had a joint detail which consisted of 4-#3 vertical bars, 24 inches long, placed in the courses above and below the slab. #4 bent bars were placed around the vertical bars and in the slab cores.

The construction sequence was the same as for Type C specimens with the exception that the joint reinforcment was placed before grouting.

3.2.2.5 Type E Specimens

The four Type E specimens consisted of wall segments 47.625 inches wide, reinforced with 4-#3, bars supporting 8

inch precast slabs at their mid-height.

The construction sequence was as follows:

a. The bottom seven courses of the walls were laid.

b. The vertical reinforcing bars were placed and grout was vibrated into the reinforced cores to the top of the sixth course.

c. The precast slab was placed on the wall and the slab blocks were laid.

d. #4 bent bars were placed around the vertical steel and in the slab cores. Grout was vibrated into the slab and the seventh course of the wall. Styrofoam was placed in the slab cores to prevent the grout from reaching more than 13 inches into the slab.

e. The next seven courses of the walls were laid and grout was vibrated into the reinforced cores.

Joint details for Types C, D and E walls are shown in Fig. 3.5. After construction was completed the specimens were moistened periodically to counteract the low relative humidity in the lab.

3.3 Loading Apparatus

The walls of the specimens were loaded in compression through a channel-roller system shown in Fig. 3.6. This system was used to simulate a pin-ended condition representing points of zero moment in the real structure. The vertical load on the walls was applied by an MTS hydraulic testing machine with a capacity of 1.5 million lbs

in compression, and the capability of maintaining a preset load to ± 10 lbs.

The vertical load on the slab was applied through two hydraulic centre pull rams connected in series. The rams had a total load capacity of 120 kips with a stroke of 5 inches. They were mounted under the 26 inch thick load floor in front of the MTS machine and were connected through a loading apparatus to a channel used to distribute the load, as a line load, on the slab. The line load was placed at 48 inches from the centre line of the wall. The weight of the loading apparatus was 225 lbs for the cast-in-place slabs and 250 lbs for the precast slabs. A diagram of the slab loading apparatus is shown in Fig. 3.7.

3.4 Instrumentation

3.4.1 Prisms

Prisms were tested in vertical compression. Vertical deformations were monitored to 1/1000 inches by the movement of the head of the MTS machine.

3.4.2 Full Scale Wall-Slab Specimens

Horizontal deflections of the walls were measured at 10 points along the height using linear variable differential transducers (LVDT's) calibrated to read in increments of 1/1000 inches. The LVDT's were mounted on an independent frame and connected to the walls with light gauge wires.

Vertical deflections of the slabs were measured at 20 inches and 36 inches from the face of the wall using LVDT's. Total axial deformations of the walls were measured by recording the vertical movement of the MTS head.

Rotations of the slab end, the block above the slab, and the block below the slab, were computed by taking the inverse sine of the difference in two adjacent LDVT measurements divided by the vertical distance between the gauge points.

The strains in the reinforcing steel in the cast-in-place slab were measured by strain gauges mounted on the reinforcement at the face of the wall. The strains in the vertical reinforcing bars were also measured by strain gauges. The gauges were mounted at one mortar joint above the slab and one mortar joint below the slab. No strain measurements were taken on the 24 inch vertical bars in the Type D walls nor was strain monitored on the #4 wrap-around bars in the precast slabs.

Vertical load on the wall was read directly from the MTS testing machine. Vertical load on the slab was measured using a 20 kip load cell. Strain gauges were mounted on the two rods used to load the slab to check that the rods were sharing the load equally.

The measuring devices (strain gauges, load cells and LVDT's) were powered by a common six-volt power supply that produced output in the range of ± .001 volts. The analog signals from the devices were converted into digital form by

a digital voltmeter controlled by an interactive Fortran program in the Nova computer. This allowed the measurements to be monitored and read into storage during testing. At a particular load level all output was measured and recorded automatically within 5 seconds. The interactive Fortran program allowed the test supervisor to determine, during the test, the increments of loading at which data was to be read and stored. After completion of testing, the data was printed on a hard copy terminal, stored on a digital casette tape and later transferred to the AMDAHL 470 computer for further processing.

A diagram of the location of LVDT's and strain gauges is shown in Fig. 3.8.

3.5 Testing Procedure

3.5.1 Prisms

All prisms were tested in axial compression. They were capped top and bottom with high strength plaster and 1/4 inch steel plates were placed so that the load was applied uniformly over the total area of the prisms.

3.5.2 Full Scale Wall-Slab Specimens

3.5.2.1 Placement of Specimen

The specimens were transported to the testing machine in a clamping device consisting of two frames connected with steel rods. The frames were placed on the two sides of the specimens and a compressive force was introduced by

tightening bolts on the rods. Rubber pads were placed at three locations on each side of the wall and two locations on each side of the slab to avoid damage. The slabs were held level as the specimens were lifted by a 10 ton overhead crane. Plate 3.1 shows a specimen being lifted.

The specimens were guided into the testing machine and set into the bottom channels which were held from rotating by temporary wedges. Plaster of paris was poured into the channels to ensure the load was distributed evenly.

Two spirit levels were used to set the slab level and the walls plumb. A stack of concrete blocks was used to temporarily support the slab until testing began. The clamping frame was then removed and the top loading channel was placed. A 3 kip load was applied to the channel to provide even set of the plaster and overall stability of the specimen. The slab loading apparatus and the measuring devices were then connected. Plate 3.2 shows a specimen ready for testing.

3.5.2.2 Application of the Loads

A sling connected to the overhead crane held the slab level while the channel wedges and the blocks supporting the slab were removed.

The wall was then loaded in increments of 10 kips to a predetermined level which varied depending on the wall. After the first 10 kips was placed on the wall the sling supporting the slab was removed. Readings on all gauges

were taken at each 10 kip increment of wall loading.

After the required axial load on the wall was reached the loading of the slab was begun. The output from the load cell was monitored and readings were taken at intervals of 0.5 to 2.0 kips up to the maximum slab load. If the walls did not become unstable at the maximum slab load then the deflections of the slab were monitored and the stroke of the centre pull rams was increased. Measurements were recorded at various intervals, as the slab deflection increased until complete instability of the walls occurred.

Table 3.1 Physical Properties of Concrete Block Units

Masonry Unit	Gross Area $in.^2$	Net Solid Area %	Compressive Strength ksi	
			Gross Area	Net Area
Stretcher	119.15	54.45	1.34	2.34
End Block	119.15	54.45	1.40	2.37
Half Block	58.15	67.00	1.58	2.27
Slab Block	11.44	100.0	2.40	2.40

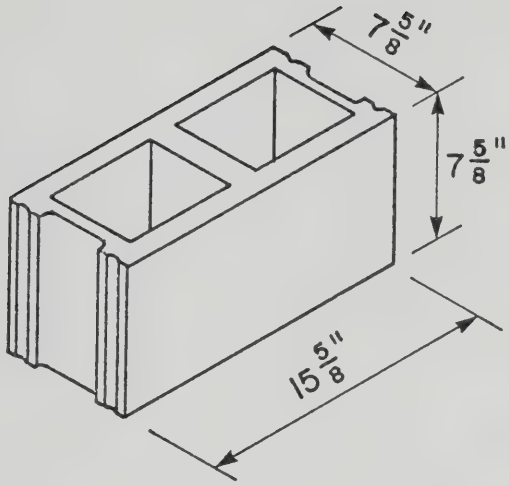

(a) stretcher

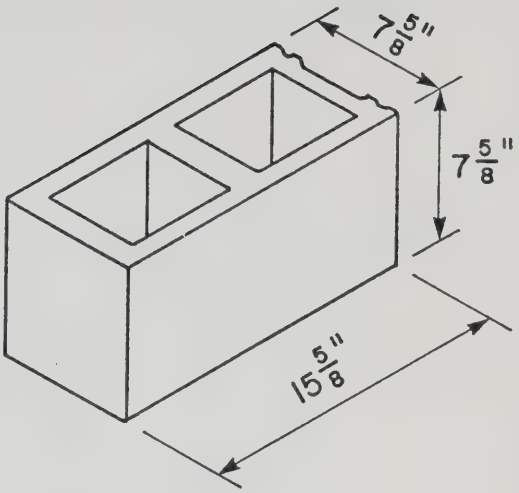

(b) single corner

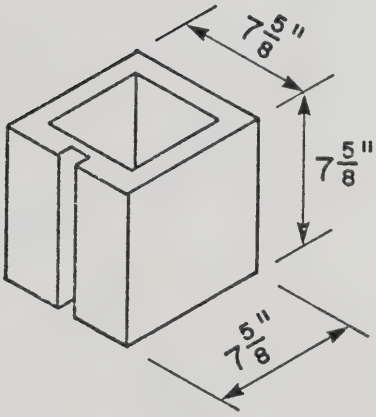

(c) half block

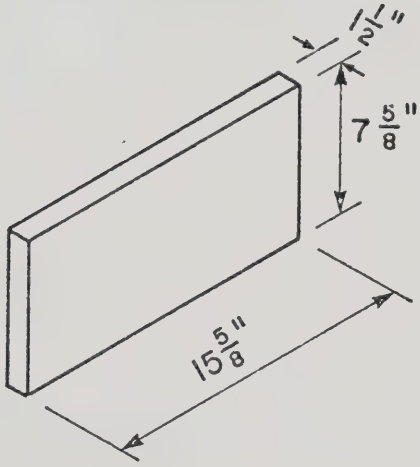

(d) slab block

Fig. 3.1 Masonry Units

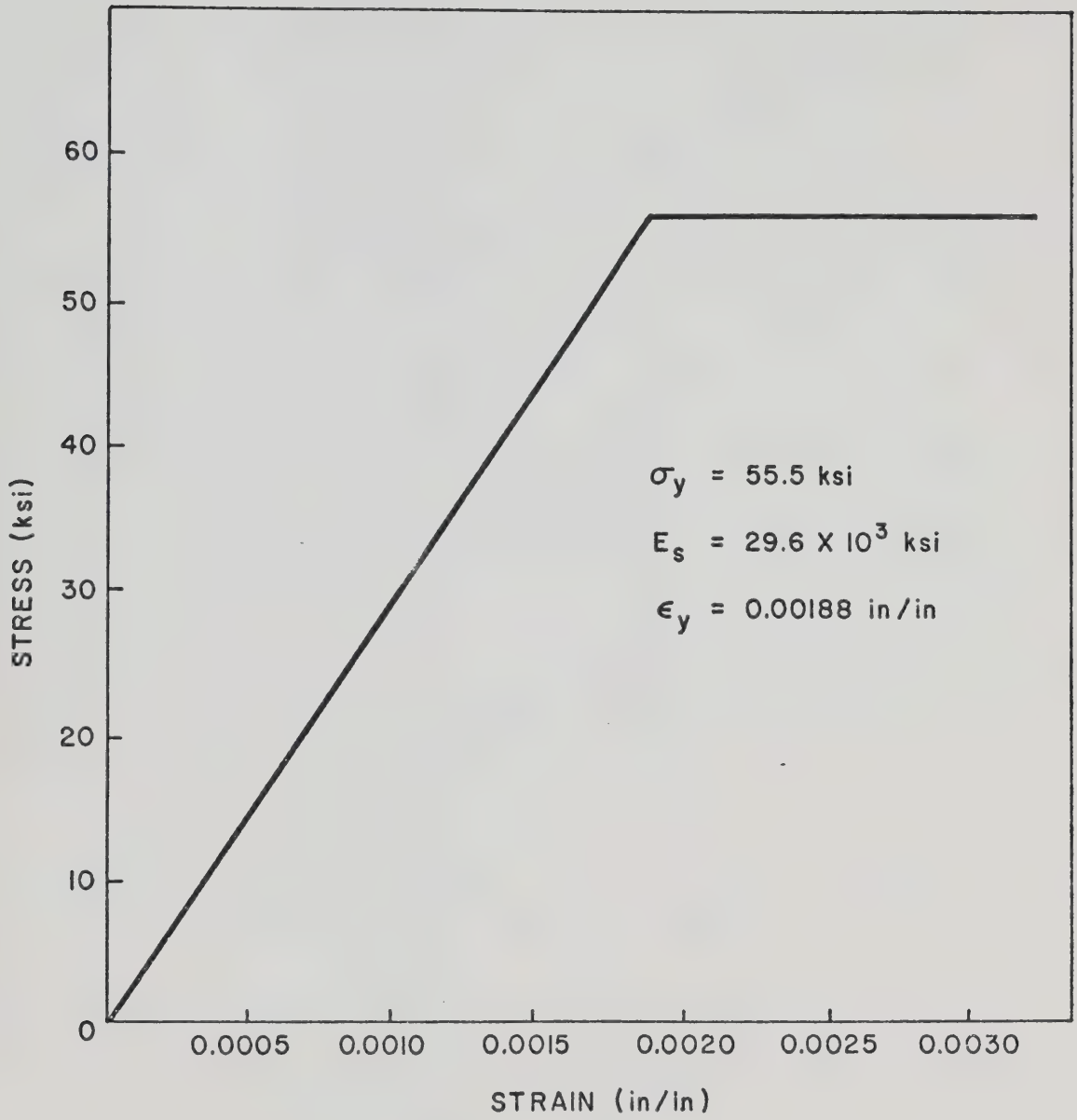

Fig. 3.2 Idealized Stress-Strain Relationship For Reinforcing Steel

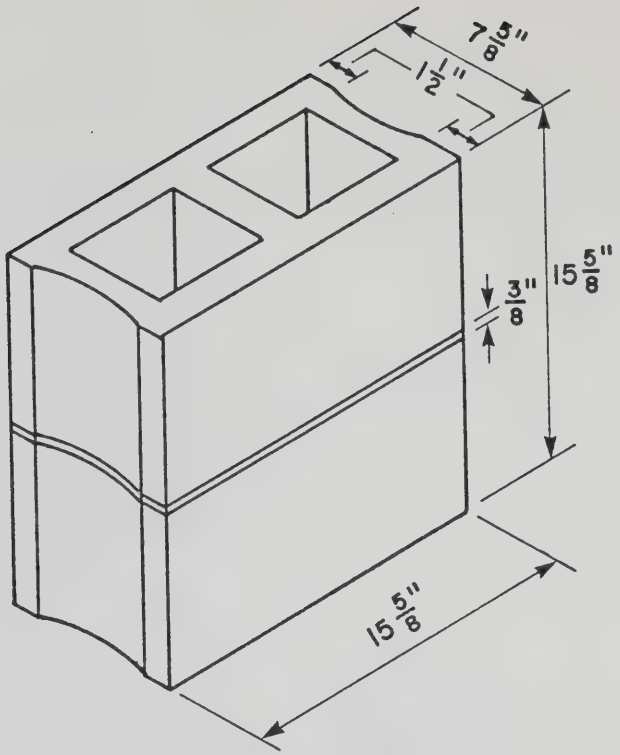

a) two block prism

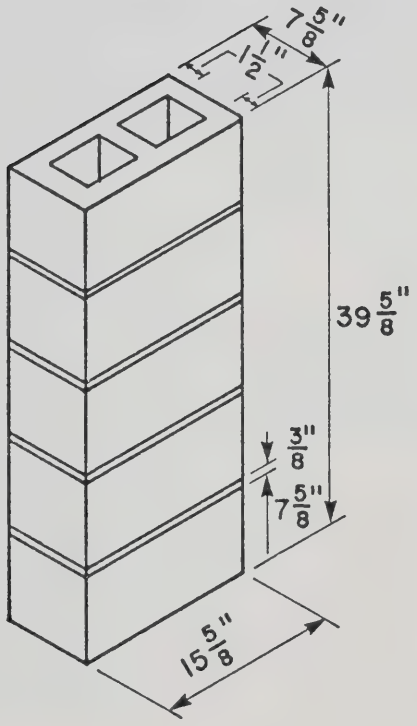

b) five block prism

Fig. 3.3 Prisms

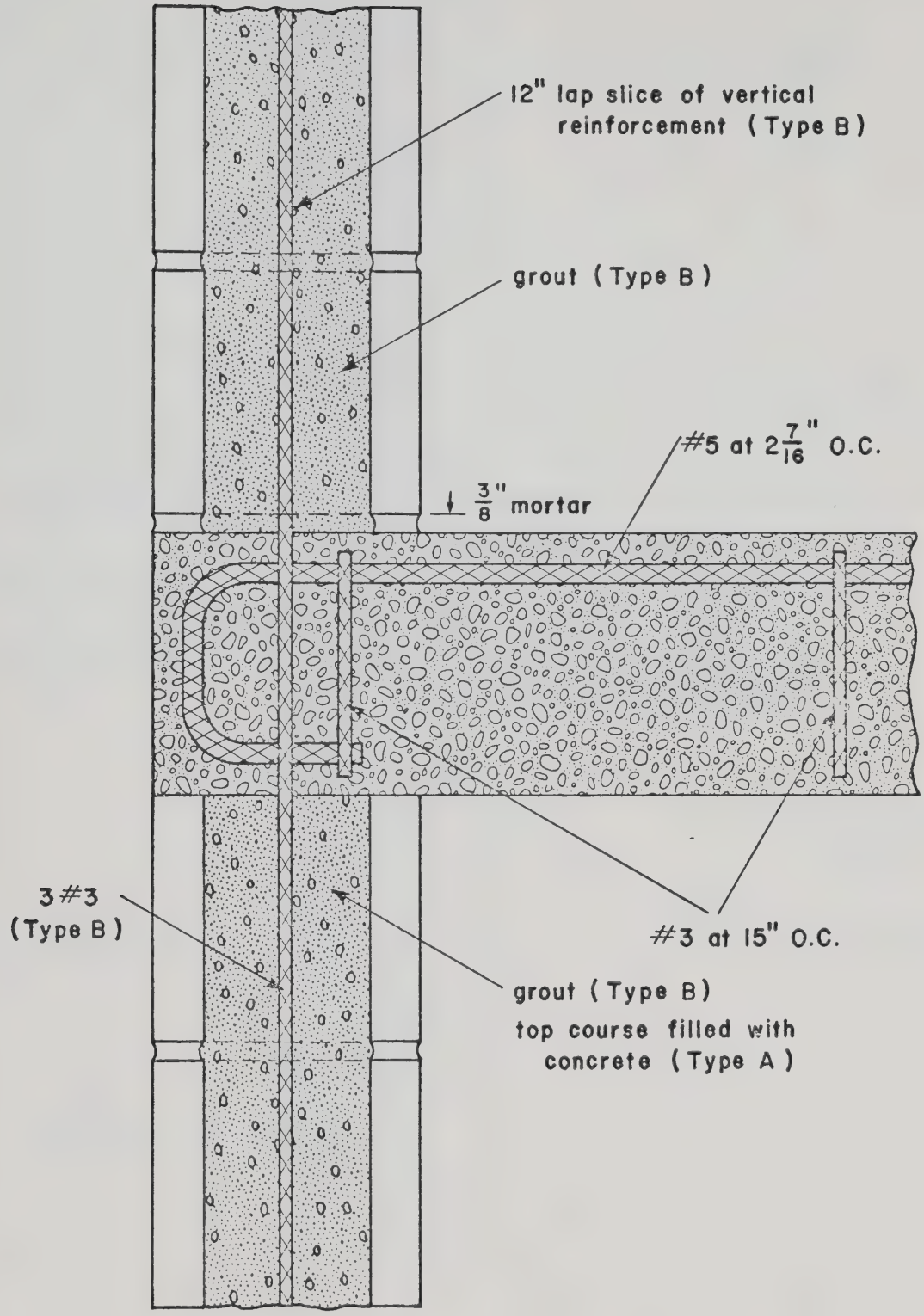

Fig. 3.4 Joint Details for Specimens A&B

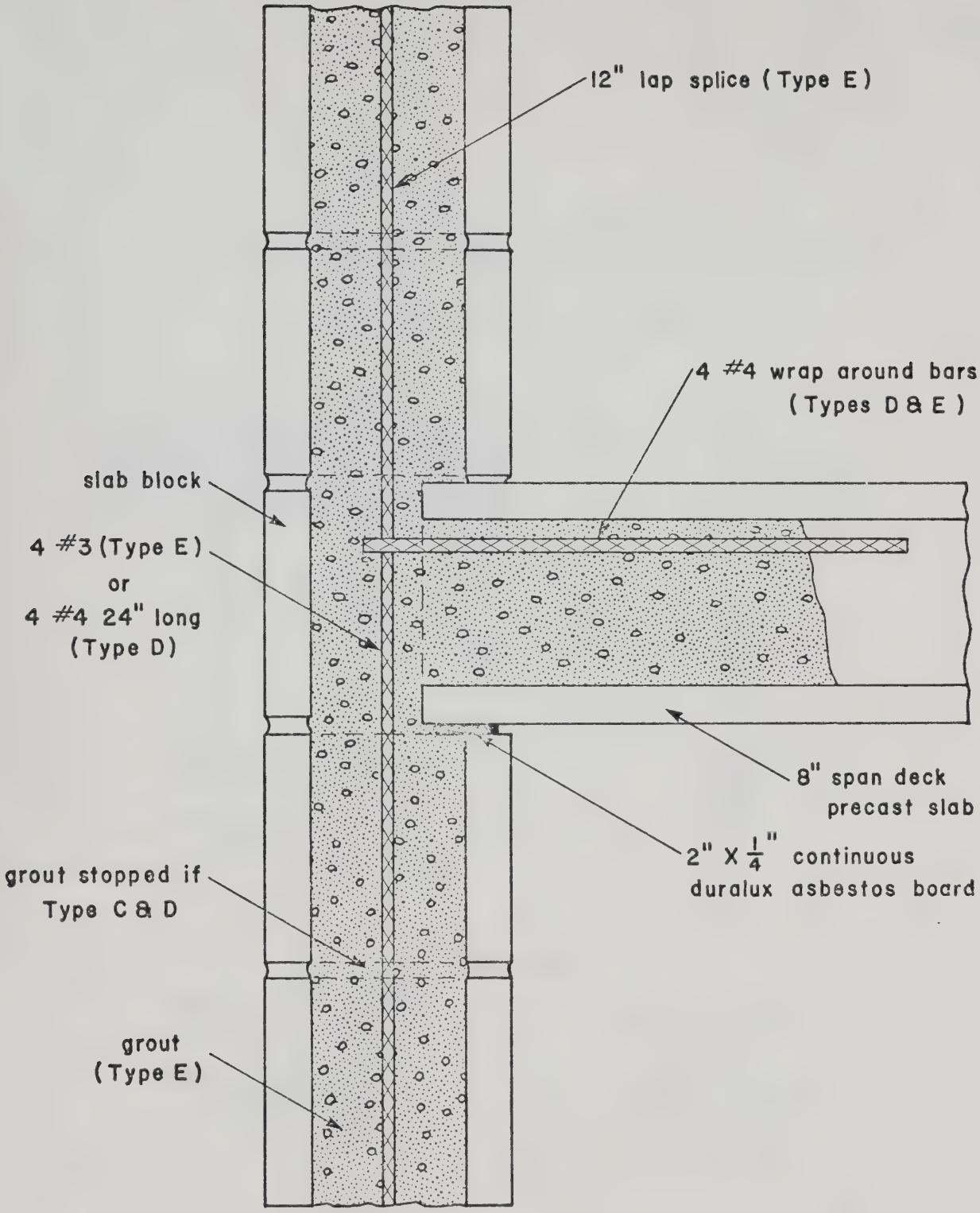

Fig. 3.5 Joint Details for Specimens C, D&E

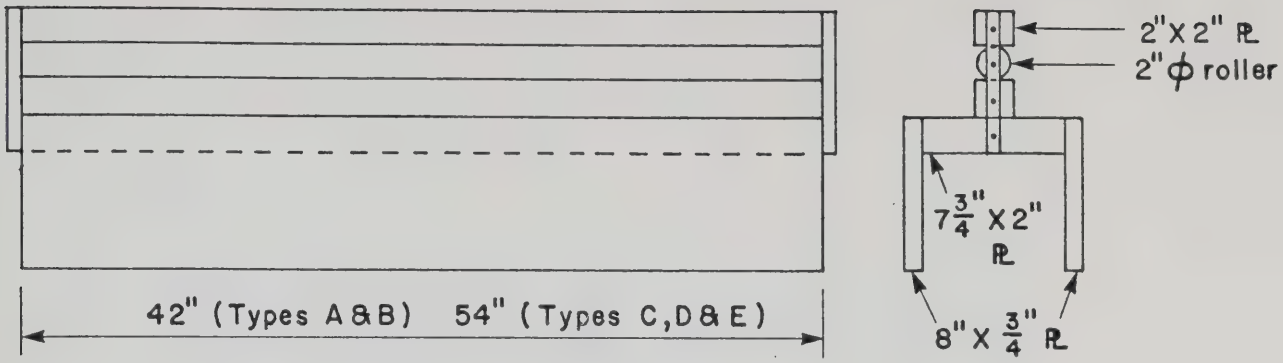

Fig. 3.6 Channel-Roller Assembly

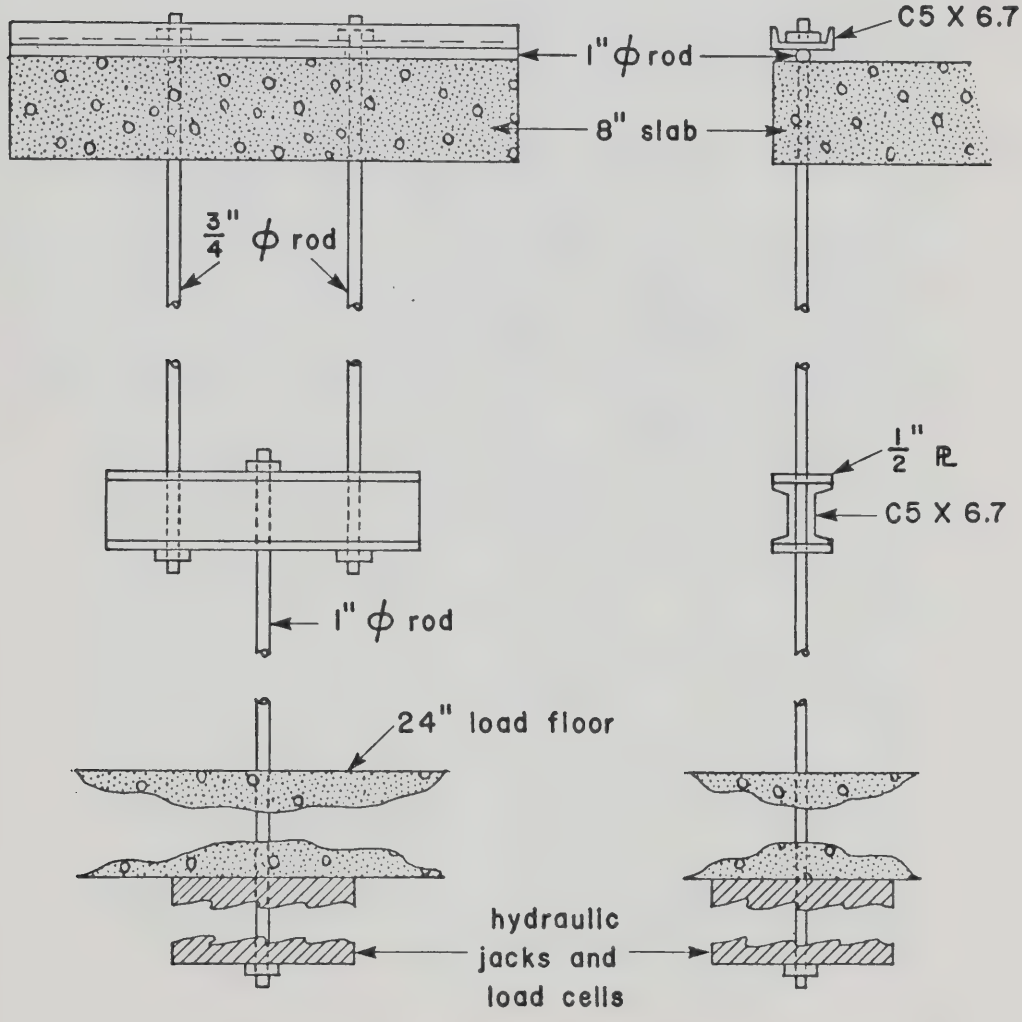

Fig. 3.7 Slab Loading Apparatus

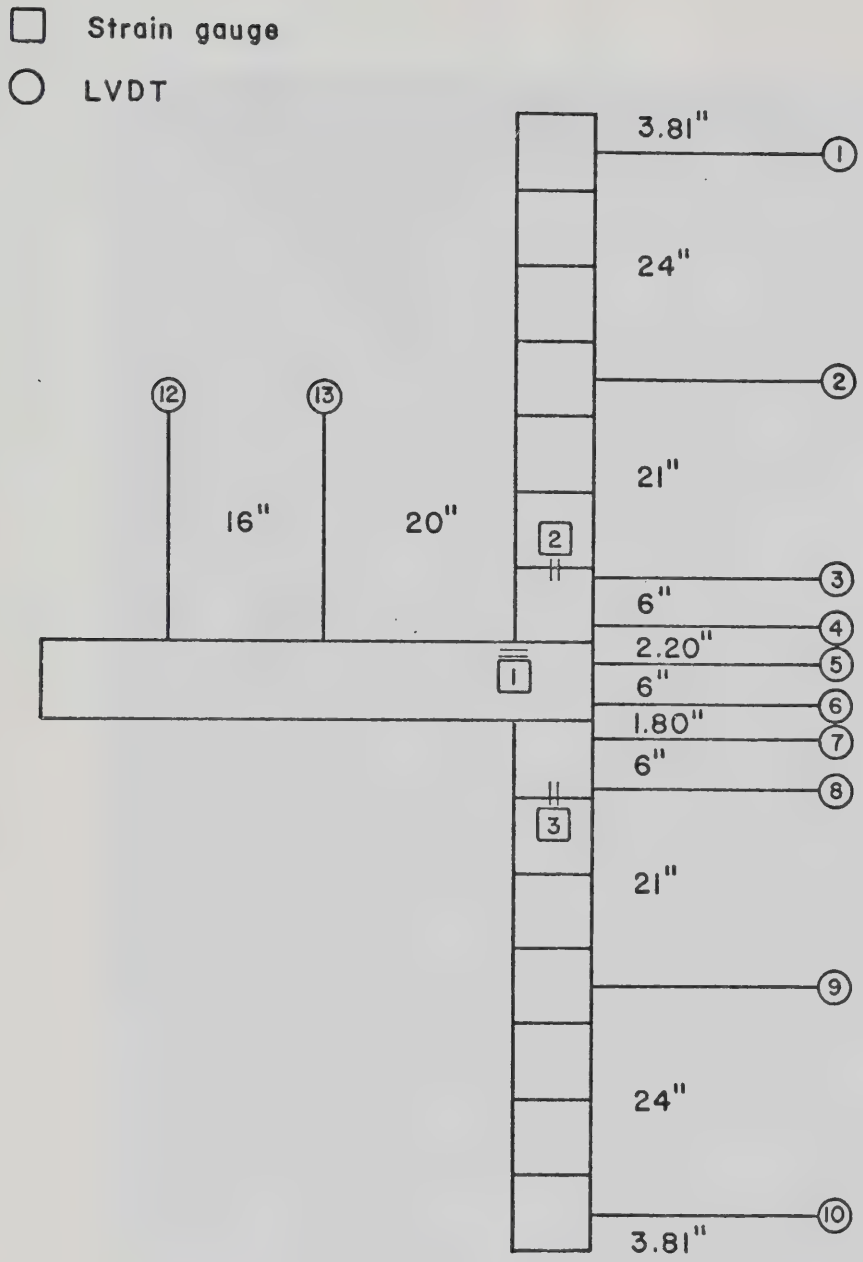

Fig. 3.8 Location of LVDT's and Strain Gauges

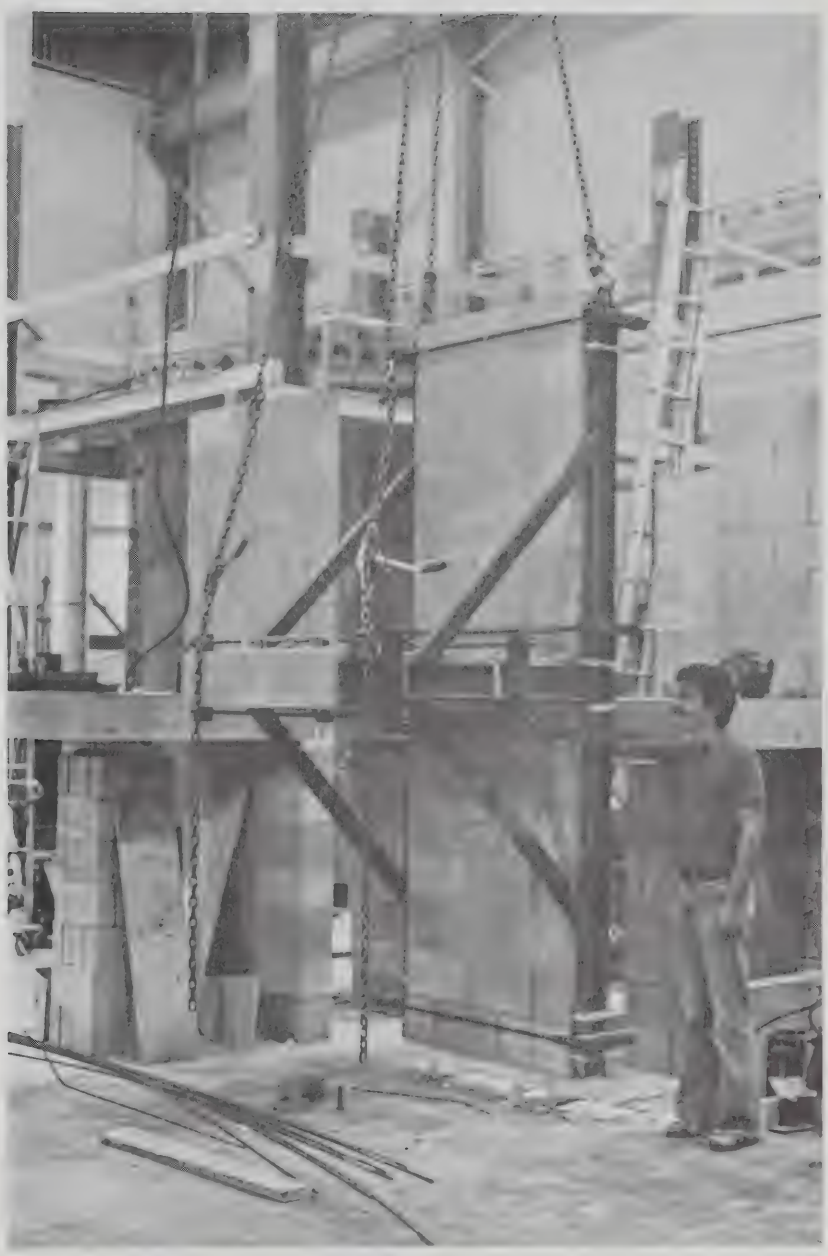

Plate 3.1 Specimen Being Transported

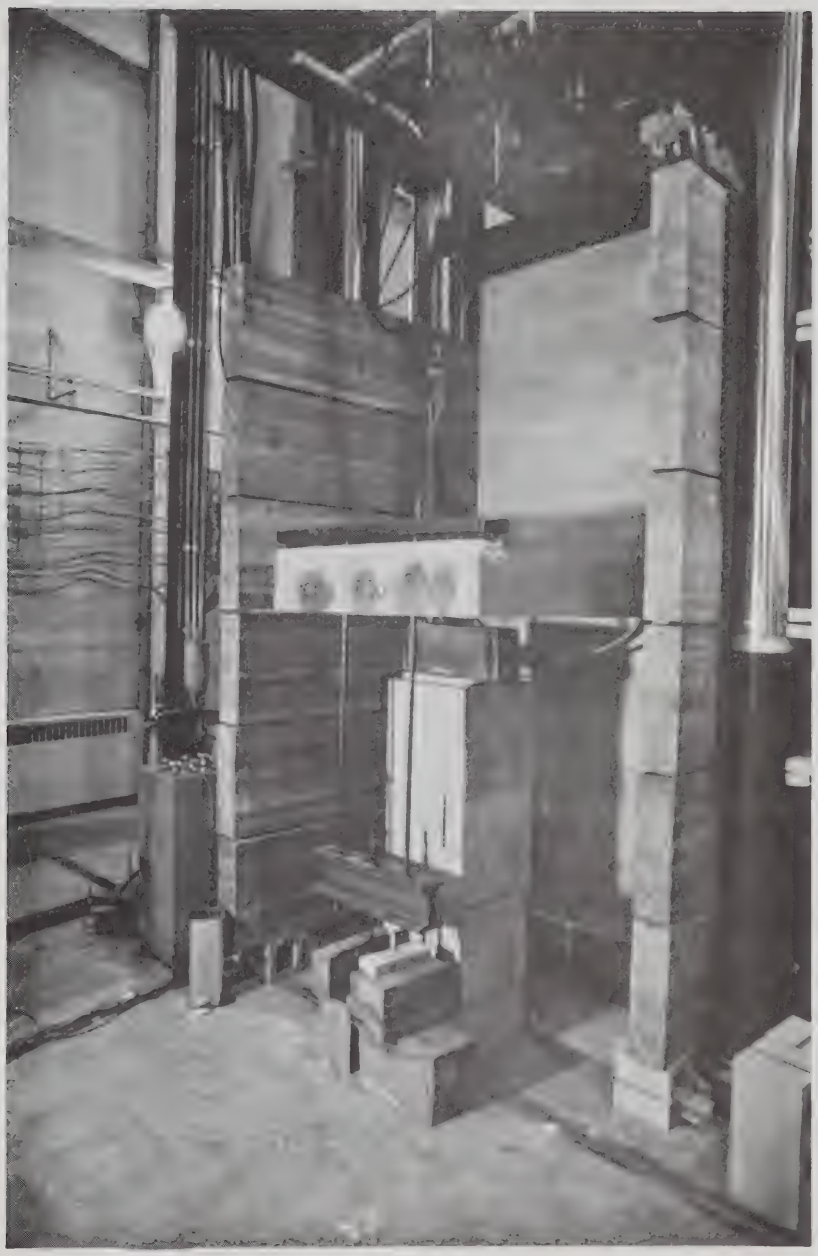

Plate 3.2 Specimen Ready for Testing

4. TEST RESULTS

4.1 Introduction

The results of the tests on prisms and full scale wall-slab specimens are summarized and presented in this chapter in tabular, graphic and photographic form.

4.2 Prisms

The five two-block prisms failed with an average compressive stress of 2015 psi. The value of f'm was determined in accordance with clause 4.3.2.3 of CSA S304 1977 "Masonry Design and Construction For Buildings " and was found to be 1722 psi.

The three five-block prisms failed with an average compressive stress of 1543 psi. The code does not allow for prisms with h/t greater than 3. However, by using the weighted average of the three tests and applying the correction factor for h/t = 3., the value for f'm was 1724 psi.

4.3 Summary of Test Results of Full Scale Wall/Slab Specimens

4.3.1 Specimens With Cast-In-Place Slabs

The cast-in-place slab specimens failed in two distinct modes depending on the magnitude of axial load on the wall. The overall failure mode was independent of whether or not

the wall was reinforced. The nature of the axial load-moment interaction of concrete masonry walls is such that walls subjected to loads higher than a certain axial load, Pb, the failure of the wall is governed by the compressive strength of the masonry. Below the balanced load the walls fail in tension. This behavior is discussed in more detail in Chapter 5. For the catagorization of tne test results of the specimens with cast-in-place slabs the walls are described as being subjected to axial loads lower or higher than Pb.

4.3.1.1 Walls Subjected To a Low Axial Load

The walls subjected to a low axial load had a tension type failure. After approximately 80% of Mmax (the maximum applied moment which the joint was able to resist) was introduced into the system, a crack opened at the mortar joint above the slab on the tension side of the wall. The size of the crack increased with increasing moment until Mmax was reached. The crack, at Mmax, was more than 1/4 in wide and the rotation of the block above the slab no longer followed the rotation of the slab end.

The deflection of the slab was then increased with the line load on the slab dropping. The deflection of the walls began to increase greatly after the maximum moment was reached. This deflection had the effect of increasing the moment on the upper wall and decreasing the moment on the lower wall. If it is assumed that 50% of the slab moment

was resisted by the upper wall, and adding the axial load-deflection (P-Delta) moment to that, the results indicate that the moment on the upper wall remained almost constant after Mmax was reached.

The deflection of the slab was finally increased until the walls became unstable and fell over under their own weight.

4.3.1.2 Walls Subjected To a High Axial Load

The walls subjected to higher axial load had a compressive failure. The moment versus slab rotation behavior was similar to that for walls subjected to lower loads until Mmax was reached.

No large tensile cracks were observed in these walls but vertical splitting cracks were found. Spalling of the mortar joint immediately above the slab on the compression face was observed as Mmax was approached. This spalling included concrete from the slab and the block above the slab.

Upon reaching Mmax the walls immediately failed. The unreinforced walls failed by vertical splitting of the upper wall extending from the slab to the top block. The reinforced walls failed by vertical splitting of only the block above the slab with the compression side of the block falling away from the specimen. For both the reinforced and unreinforced walls a large amount of concrete spalled from the slab.

The moment vs slab rotation relationships for the walls are summarized and presented graphically for unreinforced walls in Fig. 4.1 and for reinforced walls in Fig. 4.2.

A photograph of wall A25 at failure, a typical tension type failure, is presented in Plate 4.1. A photograph of wall A100 at failure, a typical compressive failure of an unreinforced wall, is presented in Plate 4.2 and a photograph of wall B150 at failure, a typical compressive failure of a reinforced wall, is presented in Plate 4.3.

4.3.2 Specimens With Precast Slabs

The failure of the wall-slab joint of the specimens with precast slabs was separate from the failure of the wall. This failure was independent of the amount of axial load applied to the wall.

All of the specimens exhibited the same type of behavior. As the slab moment was applied, the precast slab end rotated much more than that observed for the cast-in-place slabs. Even after only a small moment was introduced a vertical crack developed through the wall at the precast slab end in all specimens and this crack quickly extended over the full depth of the slab.

A large horizontal crack opened above the slab as Mmax was reached. Mmax was very small and was approximately the same for all specimens, independent of the axial load on the wall. The slab end rotated substantially as the slab moment was applied while the rotation of the wall ends was

negligible. After Mmax was reached the walls still remained stable and the rotation of the slab end could be increased with a decreasing slab moment. Although this behavior was similar to that of the cast-in-place slab specimens, the similarity was in appearance only.

The ultimate failure of the specimens, collapse or loss of stability, was different depending on the type of joint reinforcement. The slabs for the specimens with no joint reinforcement rotated to a large degree with very low loads. The crack at the slab end quickly extended up and down into the walls. Failure occurred by vertical splitting of the wall for larger axials load or, if the load on the wall was small, the slab simply rotated out of the wall. The slabs with the wrap around bars could be rotated as the moment dropped slightly until the vertical steel began to bear against the face of the wall, finally cracking the blocks.

The presence of the slab joint seriously affected the load carrying capacity of the walls. This was not neccessarily due to the introduction of a moment, as in the case for the cast-in-place slabs, but was due to the initiation of the vertical crack behind the precast slab end. This behavior is discussed later in Chapter 5.

The moment versus slab rotation relationships for all of the specimens with precast slabs are summarized in both tabular and graphic form in Appendix A. A photograph of wall D60, having a joint reinforced with wrap-around bars and two foot long vertical bars, at failure is presented in

Plate 4.4.

Table 4.1 lists the magnitude of axial load, the distance of the slab load from the centre line of the wall and indicates the degree of out of plumb of the walls for all test specimens.

4.4 Unreinforced Walls With Cast-In-Place Concrete Slabs

4.4.1 Wall A25

As the slab was loaded a horizontal crack opened in the first mortar joint above the slab. This crack became increasingly larger until Mmax was reached, at which time the crack size increased significantly and the block above the slab assumed a rotation opposite to that of the slab. The slab deflection was next increased until a large crack appeared in the mortar joint 3 blocks below the slab, and finally the bottom half of the wall tipped over. The rotations of the blocks and slab end together with the corresponding moments are tabulated in Table 4.2 and the deflected shape of the wall is presented graphically in Fig. 4.3.

4.4.2 Wall A50

As in the case for wall A25 a horizontal crack opened in the first mortar joint above the slab. The crack became larger and the mortar on the compression face of the wall began to spall off. After Mmax was reached the joint began to pry the two walls apart and eventually the bottom wall

became unstable and fell over. The rotations of the blocks and slab end with the corresponding moments are tabulated in Table 4.3 and the deflected shape of the wall is presented graphically in Fig. 4.4.

4.4.3 Wall A100

No horizontal cracks were observed until Mmax was reached and the blocks in the upper wall split vertically. The blocks in the course below the slab also split and the concrete slab spalled off, at the end of the slab reinforcing bars. The rotations of the blocks and slab end with the corresponding moments are tabulated in Table 4.4 and the deflected shape of the wall is presented graphically in Fig. 4.5.

4.4.4 Wall A150

As in the case of wall A100 no horizontal cracks were observed and at Mmax failure occurred by vertical splitting of the blocks above the slab. The blocks below the slab did not fail as with wall A100. Fig. 4.5 lists the rotations of the blocks and slab end together with the corresponding slab moments. The deflected shape of the wall is presented graphically in Fig. 4.6.

4.5 Vertically Reinforced Walls With Cast-In-Place Concrete Slabs

4.5.1 Wall B25

At Mmax a large horizontal crack opened above the slab. The crack became larger as the slab deflection was increased until the wall became unstable and tipped over. The rotations of the blocks and slab end with the corresponding moments are tabulated in Table 4.6 and Fig. 4.7 graphically depicts the deflected shape of the wall.

4.5.2 Wall B50

At 80% of Mmax a tensile crack opened in the first joint above the slab. The joint failure, at Mmax, occurred with spalling of the concrete and mortar on the compression face of the slab and spalling of the block above the slab. The deflection of the slab was then increased until the bottom wall tipped over.

The rotations of the blocks and slab end together with the corresponding moments are tabulated in Table 4.7 and the deflected shape of the wall is presented graphically in Fig. 4.8.

4.5.3 Wall B150

No horizontal cracks were observed for this specimen until Mmax was reached. At approximately 70% of Mmax a vertical crack was observed along the centre line of the wall. Failure occurred at Mmax by spalling of the mortar

and concrete around the first joint above the slab on the compression side of the wall. The walls also became unstable and the slab was able to rotate freely under its own weight.

Table 4.8 lists the rotations of the blocks and slab end along with the corresponding moments. Fig. 4.9 graphically depicts the deflected shape of the wall.

4.5.4 Wall B200

At approximately 50% of Mmax a vertical crack appeared along a mortar joint on the top half of the wall and at 70% of Mmax this crack had extended to the full height of the wall.

No further cracking occurred until approximately 90% of Mmax was reached and the concrete blocks and slab at the first mortar joint above the slab began to spall off. The failure of the specimen occurred at Mmax where all of the concrete was crushed around the first mortar joint above the slab. The slab was then able to rotate freely under its own weight.

The rotations of the blocks and the slab end together with the corresponding moments are tabulated in Table 4.9 and the deflected shape of the wall is presented graphically in Fig. 4.10.

4.6 Unreinforced Walls With Precast Concrete Slabs

4.6.1 Specimens With No Joint Reinforcement

4.6.1.1 Wall C60

Large slab deflections were measured immediately after slab loading was begun. The slab end rotated within the joint and no rotations of the wall ends were observed. At Mmax, which was quickly reached, a large vertical crack developed through the wall at the precast slab end.

After Mmax was reached the slab deflections increased rapidly with very little load until the slab began to rotate out of the joint under its own weight. The slab was then lifted back to its original position and, because the wall was undisturbed except for the crack at the slab end, the axial load on the wall was increased until the wall failed. Increasing the axial load on the wall caused the vertical crack at the slab end to extend through the full height of the wall. The wall failed at 120 kips by splitting along the extended vertical crack.

4.6.1.2 Wall C120

No measurements were taken after the slab loading began because the wall failed at a very small applied moment. As soon as the slab supports were removed a vertical crack developed through the wall at the precast slab end. A very small load (.7 kip) was placed on the slab when the crack suddenly extended and the wall failed by splitting vertically.

4.6.2 Specimens With Joint Reinforcement

4.6.2.1 Wall D60

A large slab deflection occurred as soon as the slab supports were removed. As Mmax was reached a vertical crack opened at the precast slab end and a horizontal crack appeared along the mortar joint at the top of the slab. The deflection of the slab was increased and the joint was able to resist some moment. This continued until the tops of the vertical bars began pushing through the face of the wall.

Next, the slab was lifted to its original position and the axial load on the wall was increased. The wall failed, under an axial load of 140 kips, by crushing and spalling of the blocks where the vertical bars had been pushing through.

4.6.2.2 Wall D120

As with wall D60, a vertical crack occurred at the precast slab end as Mmax was reached and the deflection of the slab was increased while the wall-slab joint resisted some moment. Eventually vertical cracks appeared, on the face of the wall, at the location of the vertical reinforcing bars. The bars began pushing through the face of the wall and the test was terminated.

4.7 Vertically Reinforced Walls With Precast Slabs

4.7.1 Wall E60

As with wall D60 a vertical crack at the precast slab end accompanied Mmax. The horizontal crack in the mortar

joint above the slab also appeared at this time.

The deflection of the slab was increased further and the joint was able to resist a small applied moment. The vertical crack began extending into the blocks above and below the slab and eventually extended through the entire height of the wall. Some spalling of the blocks immediately below the slab occurred. Failure was caused by spalling of all of the blocks in the two courses above the slab on the slab face of the wall.

4.7.2 Wall E120

A vertical crack at the precast slab end occurred as Mmax was reached. Increasing the deflection of the slab caused the crack to extend into the blocks above the slab.

After considerable deflection of the slab was attained, the slab was leveled and the axial load on the wall was increased to 250 kips, the maximum allowed in the preset load range of the MTS machine. When this axial load was reached the slab supports were removed. The weight of the slab caused sufficient rotation of the slab end to initiate failure of the wall. This failure was similar to the spalling failure of wall E60.

4.7.3 Wall E250

As with the previous tests, a vertical crack developed through the wall at the precast slab end. However, this occurred with only a small amount of moment. As the moment

was increased the vertical crack extended to the full depth of the joint and into the block above the slab. Mmax was lower than in previous tests, although all of these moments were quite small. The deflection of the slab was increased until failure occurred. The type of failure was the same as for walls E60 and E120.

4.7.4 Wall E350

Because of the similarities of all of the previous failures and the indication that the presence of the joint lowered the axial load capacity of the wall, it was decided to test this last specimen under axial load only. The slab supports were removed, thus there was a small moment at the joint caused by the weight of the slab.

As the axial load on the wall increased random vertical cracks appeared. Eventually a vertical crack initiated at the precast slab end. This vertical crack soon opened and failure of the wall occurred by splitting of the wall and spalling of the blocks as in the previous wall failures.

Table 4.1 Loading Details For Test Specimens

Specimen Number	Axial Load kips	Eccentricity[1] in	Out Of Plumb[2] in
A25	25	47.00	+1/2
A50	50	47.50	PLUMB
A100	100	47.00	PLUMB
A150	150	47.00	PLUMB
B25	25	48.25	+1/2
B50	50	47.75	+3/8
B150	150	47.25	PLUMB
B200	200	47.75	PLUMB
C60	60	46.75	PLUMB
C120	120	46.75	-1/4
D60	60	46.75	-3/8
D120	120	46.75	-3/8
E60	60	46.75	-3/8
E120	120	46.75	-5/8
E250	250	46.75	-1/4
E350	350	0.00	-1/4

1. The eccentricity is the distance from the line load on the slab to the centre line of the wall.
2. A positive out of plumb indicates that the top of the wall leaned towards the slab.

Table 4.2 Moments and Rotations For Wall A25

Incr No.	Mslab Kip-In	Mu Kip-In	θvl Degrees	θh Degrees	θvu Degrees	θhdef Degrees
2	0.	0.	0.01	0.02	-0.07	-0.06
3	35.	18.	0.02	0.02	-0.07	-0.06
4	91.	47.	0.02	-0.02	-0.03	-0.04
5	110.	55.	-0.01	-0.02	-0.03	-0.03
6	146.	74.	0.00	0.03	-0.02	0.00
7	158.	86.	0.17	0.16	-0.22	0.25
8	149.	86.	0.23	0.31	-0.35	0.41
9	141.	86.	0.21	0.50	-0.50	0.59
10	117.	83.	0.40	0.68	-0.83	0.96
11	108.	82.	0.41	0.81	-0.95	1.14
12	98.	81.	0.47	0.91	-1.11	1.29
13	90.	81.	0.27	----	-1.22	1.44
14	83.	80.	0.39	----	-1.32	1.55
15	72.	79.	0.58	----	-1.51	1.75
16	53.	77.	0.66	----	-1.81	2.07

Table 4.3 Moments and Rotations For Wall A50

Incr No.	Mslab Kip-In	Mu Kip-In	θvl Degrees	θh Degrees	θvu Degrees	θhdef Degrees
2	35.	20.	-0.04	0.03	0.01	----
3	35.	21.	-0.02	0.01	0.00	-0.03
4	77.	42.	-0.03	0.03	0.01	-0.01
5	130.	69.	-0.01	0.05	0.03	0.02
6	179.	94.	-0.01	0.08	0.04	0.04
7	236.	123.	0.02	0.09	0.06	0.06
8	259.	135.	0.04	0.11	0.07	0.08
9	300.	158.	0.06	0.16	0.04	0.13
10	323.	174.	0.07	0.24	-0.01	0.21
11	320.	180.	0.14	0.32	-0.13	0.33
12	308.	181.	0.24	0.37	-0.28	0.45
14	281.	181.	0.48	0.55	-0.57	0.69
15	263.	181.	0.57	0.67	-0.70	0.93
16	243.	180.	0.69	0.76	-0.89	1.01
17	219.	178.	0.84	0.96	-1.13	1.31
19	187.	176.	1.13	1.19	----	----
20	168.	175.	1.20	1.28	----	----
21	152.	173.	1.81	1.38	-1.48	----
24	107.	----	----	----	----	----

Table 4.4 Moments and Rotations For Wall A100

Incr No.	Mslab Kip-In	Mu Kip-In	θvl Degrees	θh Degrees	θvu Degrees	θhdef Degrees
10	0.	-3.	-0.04	-0.17	-0.01	-0.11
11	35.	16.	-0.21	-0.15	0.04	-0.08
12	97.	48.	-0.01	-0.13	0.04	-0.07
13	149.	74.	0.01	-0.09	0.04	-0.06
14	283.	144.	0.07	-0.04	0.06	0.00
15	367.	188.	0.10	0.01	0.09	0.04
16	474.	245.	0.16	0.08	0.08	0.12
17	595.	320.	0.32	0.26	0.01	0.34
18	518.	302.	0.45	0.27	-0.15	0.63
19	478.	291.	0.52	0.26	-0.22	0.75

Table 4.5 Moments and Rotations For Wall A150

Incr No.	Mslab Kip-In	Mu Kip-In	θvl Degrees	θh Degrees	θvu Degrees	θhdef Degrees
8	35.	27.	-0.02	----	-0.06	-0.07
9	147.	87.	-0.01	----	-0.02	-0.02
10	251.	140.	0.02	----	0.01	0.02
11	300.	166.	0.05	----	0.03	0.05
12	376.	206.	0.08	----	0.04	0.08
13	456.	248.	0.17	----	0.04	0.11
14	537.	291.	0.15	----	0.04	0.17
15	563.	306.	0.16	----	0.04	0.19
16	592.	322.	0.18	----	0.03	0.22
17	630.	344.	0.22	----	0.03	0.27
18	669.	365.	----	----	----	0.30

Table 4.6 Moments and Rotations For Wall B25

Incr No.	Mslab Kip-In	Mu Kip-In	θvl Degrees	θh Degrees	θvu Degrees	θhdef Degrees
3	35.	17.	-0.03	-0.03	-0.09	-0.04
4	63.	31.	-0.02	-0.02	-0.05	-0.04
5	99.	50.	0.00	0.00	0.02	-0.03
6	141.	71.	0.02	0.02	0.02	0.00
7	161.	82.	0.04	0.03	0.01	0.02
8	179.	91.	0.06	0.05	0.02	0.05
9	212.	108.	0.11	0.06	0.02	0.09
10	243.	125.	0.14	0.08	0.05	0.16
11	270.	141.	0.17	0.13	0.05	0.23
12	278.	146.	0.20	0.17	0.02	0.26
13	267.	146.	0.34	0.37	-0.22	0.50
15	265.	153.	0.69	0.49	-0.51	0.90
17	256.	160.	1.14	0.86	-0.94	1.40
19	229.	159.	1.52	----	-1.52	2.02
21	185.	152.	2.02	----	-2.18	----
23	157.	147.	2.25	----	-2.58	----
25	131.	146.	0.53	----	-3.12	-3.12
27	94.	142.	-4.20	----	-3.81	----
28	84.	140.	----	----	----	----

Table 4.7 Moments and Rotations For Wall B50

Incr No.	Mslab Kip-In	Mu Kip-In	θvl Degrees	θh Degrees	θvu Degrees	θhdef Degrees
3	45.	23.	0.04	0.00	0.24	0.06
4	100.	50.	0.06	0.09	0.34	0.09
5	151.	76.	0.08	0.11	0.38	0.11
6	196.	99.	0.09	0.14	0.39	0.13
7	261.	132.	0.11	0.15	0.38	0.16
8	309.	157.	0.12	0.18	0.38	0.21
9	358.	184.	0.13	0.21	0.36	0.26
10	390.	203.	0.15	0.24	0.32	0.32
11	402.	210.	0.17	0.25	0.32	0.37
12	423.	224.	0.18	0.28	0.30	0.44
13	443.	249.	0.35	0.34	0.18	0.81
14	417.	248.	0.47	----	-0.03	----
15	399.	249.	0.53	----	-0.09	----
16	382.	250.	0.66	----	-0.33	----
17	354.	251.	0.87	----	-0.47	----
18	319.	245.	0.99	----	-0.68	----
19	278.	237.	1.18	----	----	----
20	233.	223.	1.67	----	----	----
21	158.	208.	1.77	----	----	----

Table 4.8 Moments and Rotations For Wall B150

Incr No.	Mslab Kip-In	Mu Kip-In	θvl Degrees	θh Degrees	θvu Degrees	θhdef Degrees
5	35.	17.	0.04	-0.03	-0.09	-0.03
6	168.	82.	0.04	-0.03	0.00	0.03
7	247.	122.	0.04	0.01	0.09	0.05
8	318.	159.	0.04	0.10	0.13	0.08
9	412.	208.	0.09	0.14	0.17	0.13
10	509.	258.	0.12	0.18	0.19	0.14
11	560.	285.	0.14	0.21	0.19	0.17
12	604.	308.	0.15	0.22	0.21	0.19
13	651.	333.	0.16	0.24	0.22	0.24
14	691.	355.	0.19	0.26	0.22	0.29
15	746.	388.	0.22	0.31	0.23	0.38
16	788.	412.	0.25	0.35	0.22	0.43
17	822.	432.	0.26	0.37	0.22	0.47
18	852.	449.	0.28	0.40	0.23	0.50
19	886.	471.	0.32	0.46	0.23	0.57
20	912.	489.	0.35	0.51	0.23	0.62
21	935.	504.	0.37	0.55	0.24	0.66
22	964.	537.	0.44	0.65	0.20	0.79
23	940.	552.	----	----	----	----

Table 4.9 Moments and Rotations For Wall B200

Incr No.	Mslab Kip-In	Mu Kip-In	θvl Degrees	θh Degrees	θvu Degrees	θhdef Degrees
6	46.	26.	-0.02	-0.30	0.08	-0.32
7	138.	74.	0.00	-0.26	0.09	-0.30
8	243.	128.	0.03	-0.24	0.14	-0.25
9	328.	174.	0.04	-0.19	0.16	-0.22
10	430.	228.	0.07	-0.17	0.16	-0.17
11	473.	250.	0.09	-0.16	0.19	-0.15
12	520.	276.	0.10	-0.14	0.18	-0.13
13	577.	306.	0.12	-0.11	0.19	-0.10
14	618.	328.	0.13	-0.10	0.21	-0.07
15	683.	364.	0.15	-0.06	0.21	-0.02
16	713.	383.	0.18	-0.03	0.20	0.01
17	753.	408.	0.20	-0.01	0.21	0.06
18	781.	429.	0.23	0.02	0.21	0.12
19	818.	452.	0.25	0.03	0.18	0.15
20	855.	483.	0.30	0.07	0.18	0.23
21	890.	525.	0.41	0.11	0.16	0.36

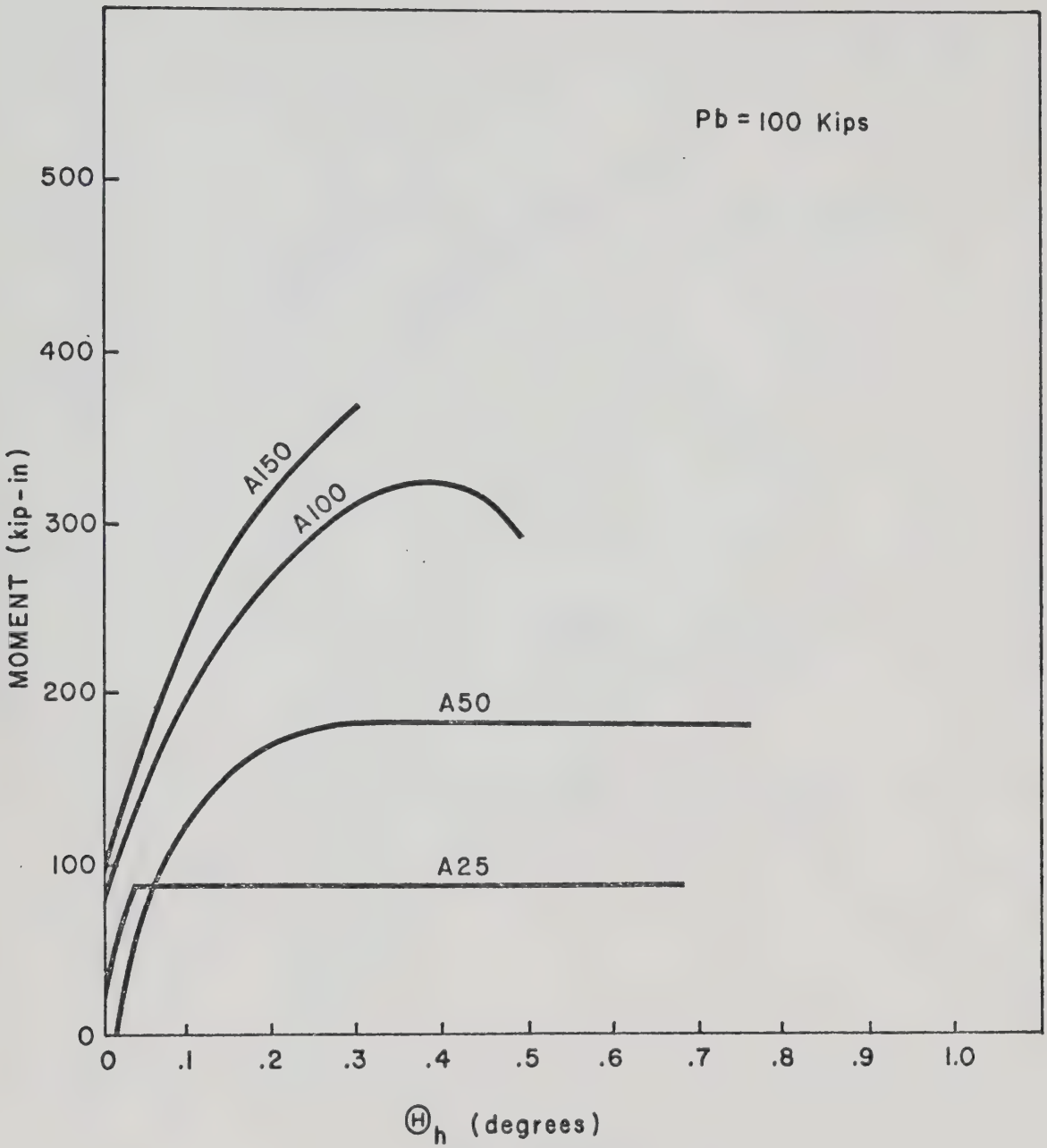

Fig. 4.1 Moments vs Slab Rotations For Unreinforced Walls

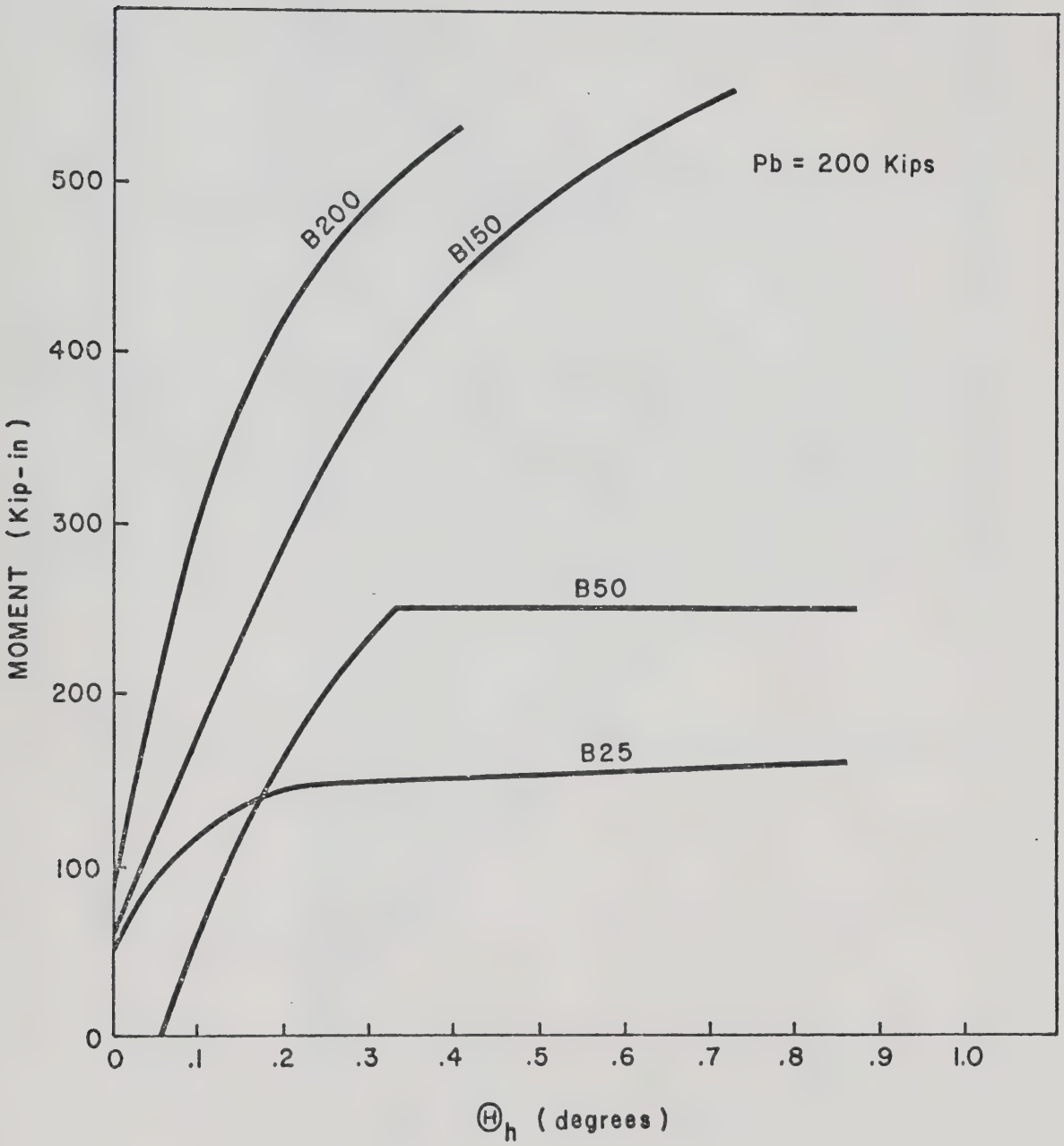

Fig. 4.2 Moments vs Slab Rotations For Reinforced Walls

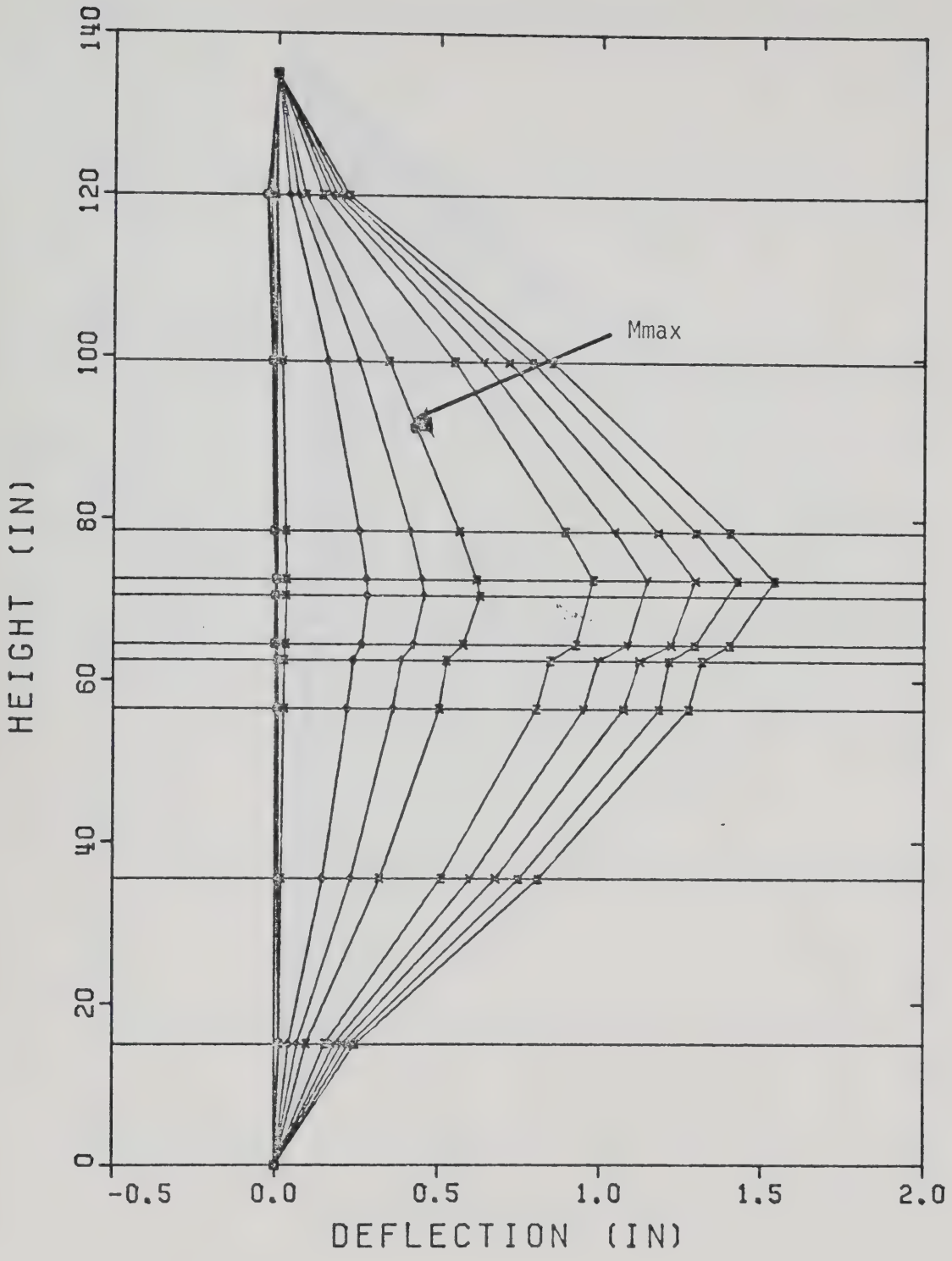

Fig. 4.3 Deflected Shape Of Wall A25

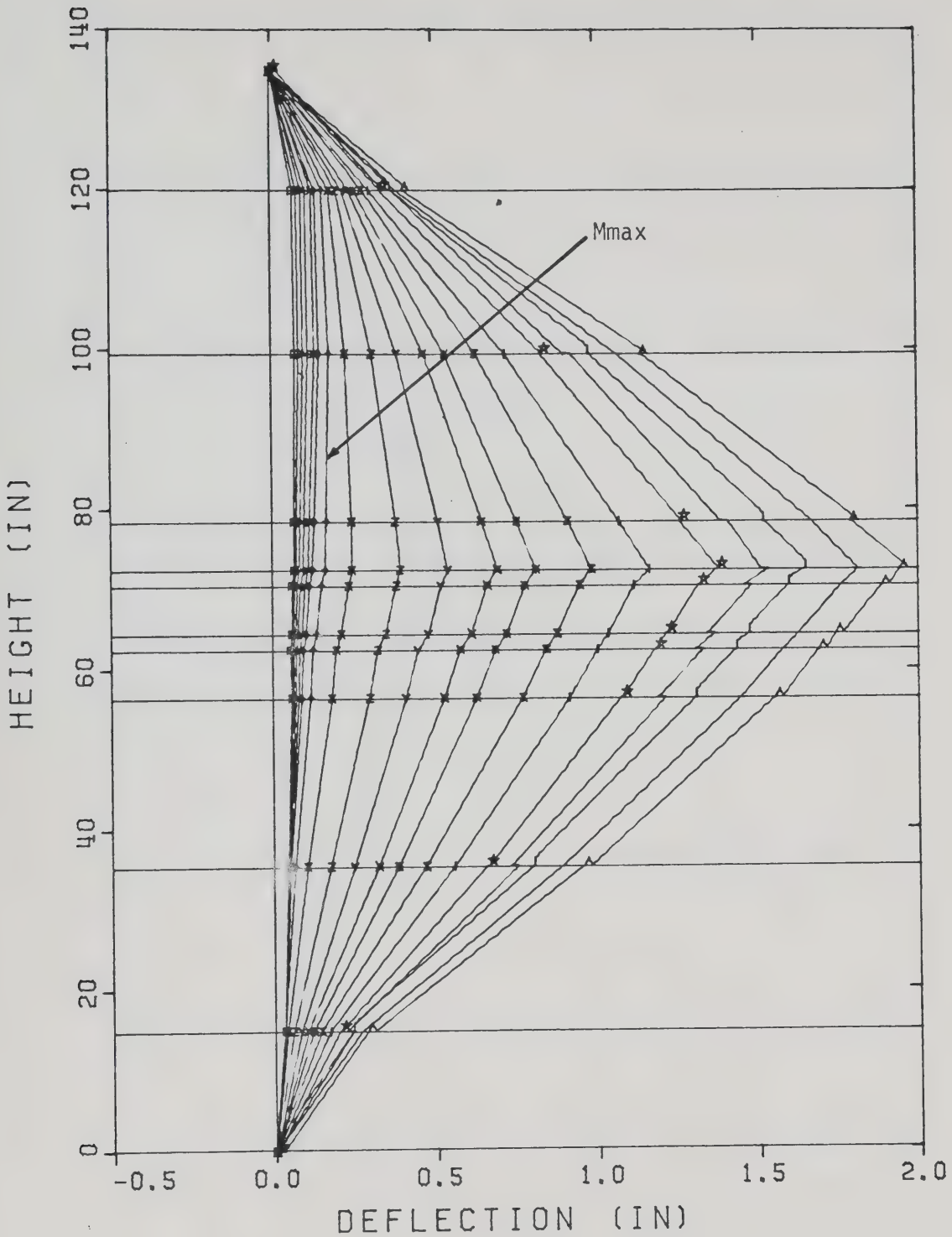

Fig. 4.4 Deflected Shape Of Wall A50

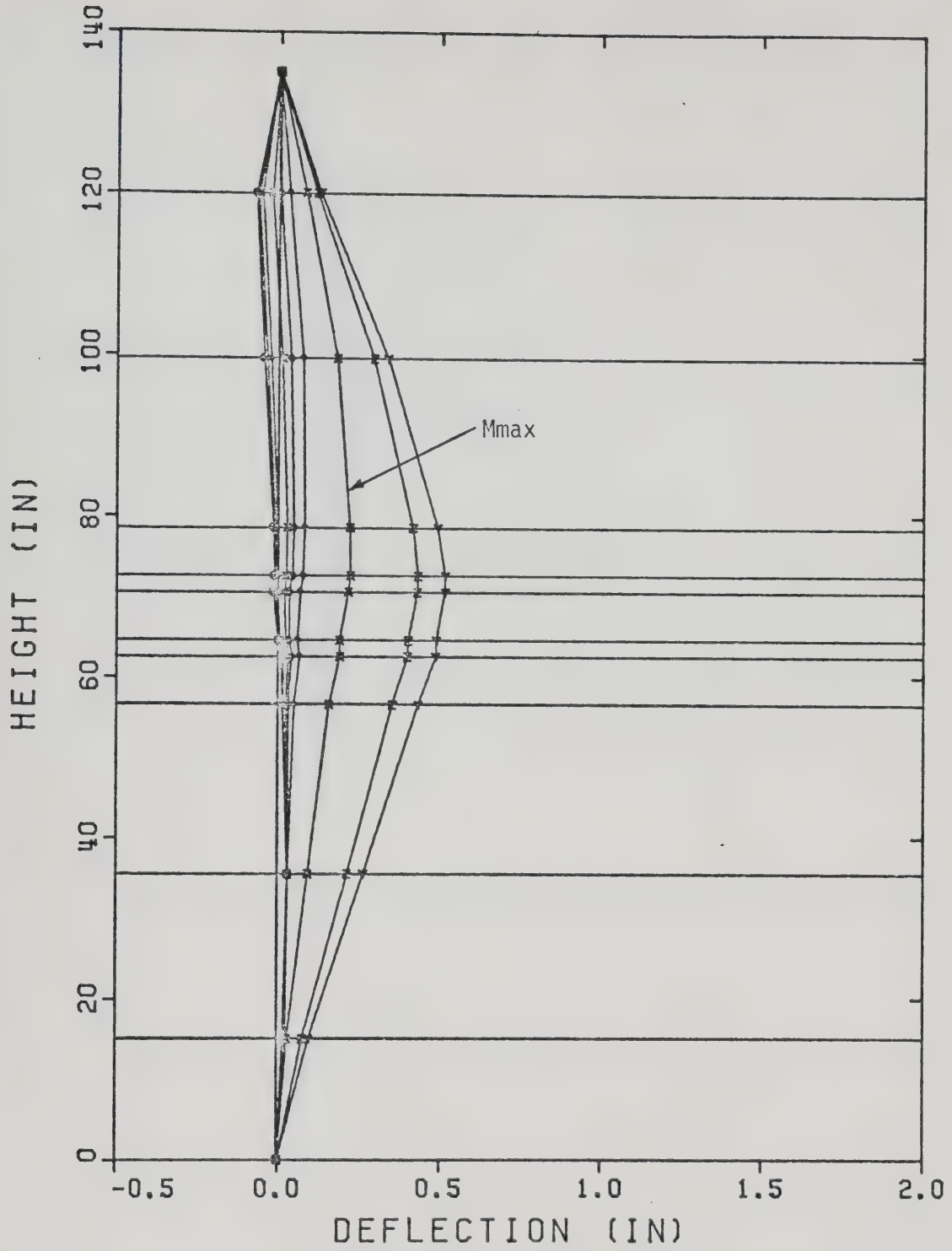

Fig. 4.5 Deflected Shape Of Wall A100

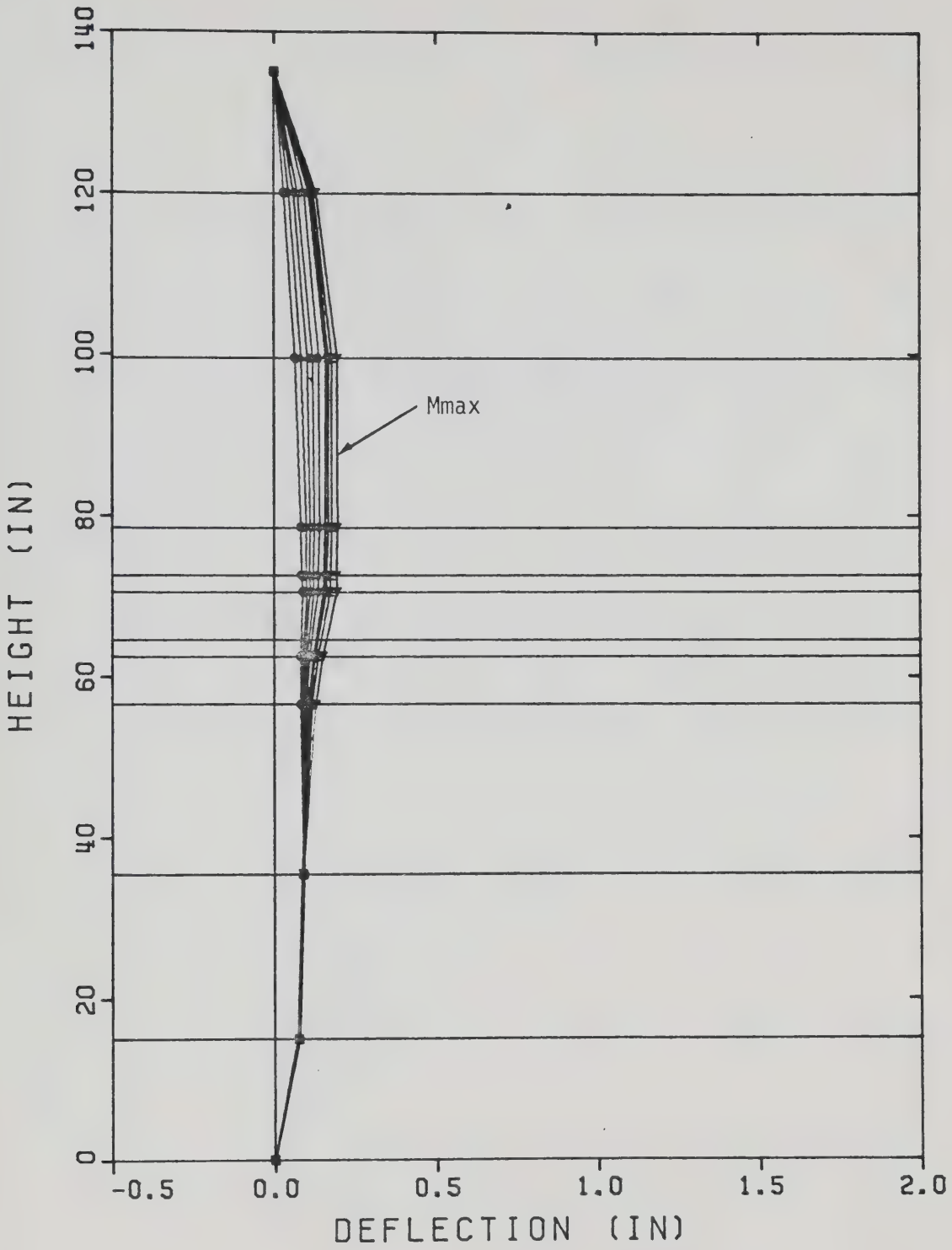

Fig. 4.6 Deflected Shape Of Wall A150

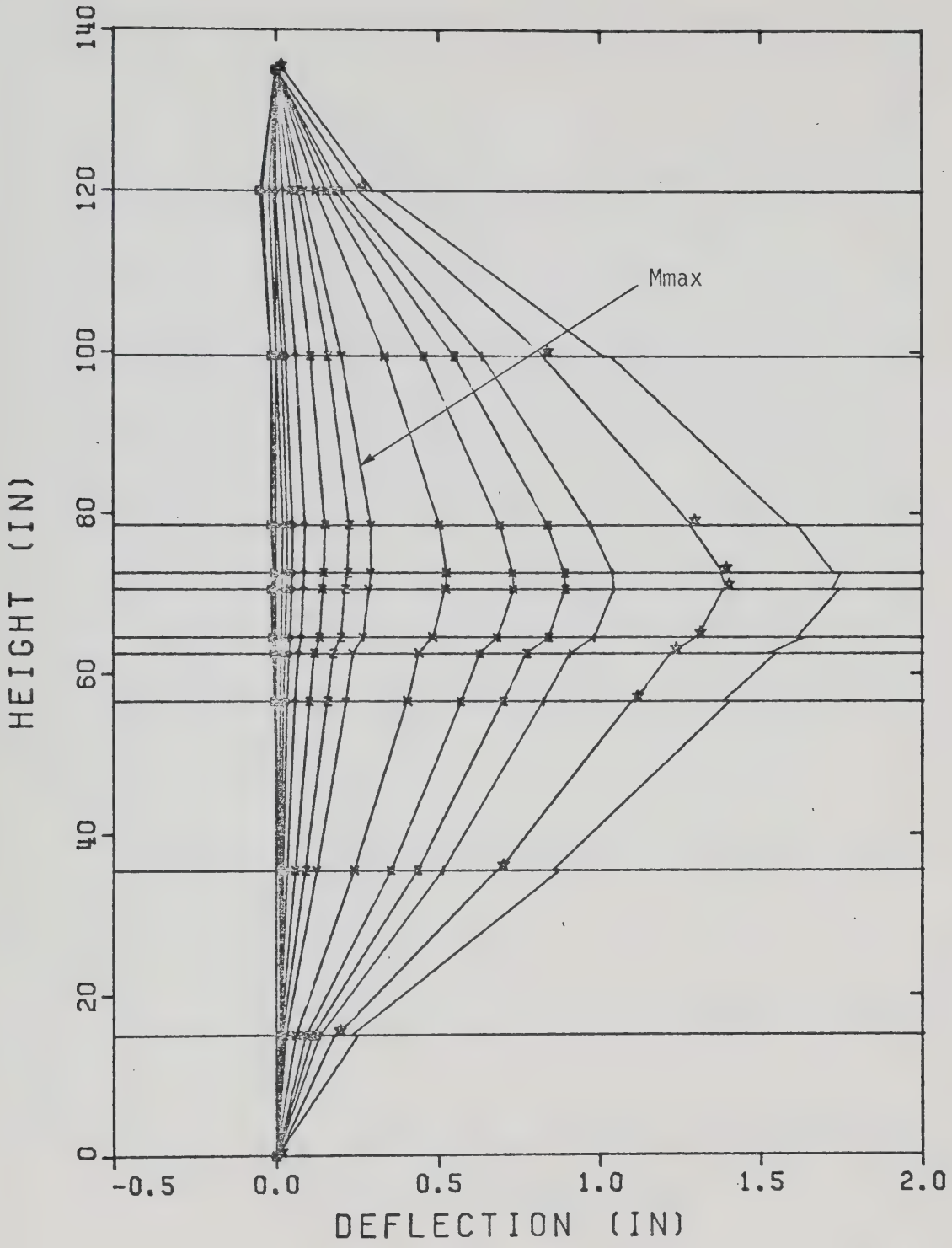

Fig. 4.7 Deflected Shape Of Wall B25

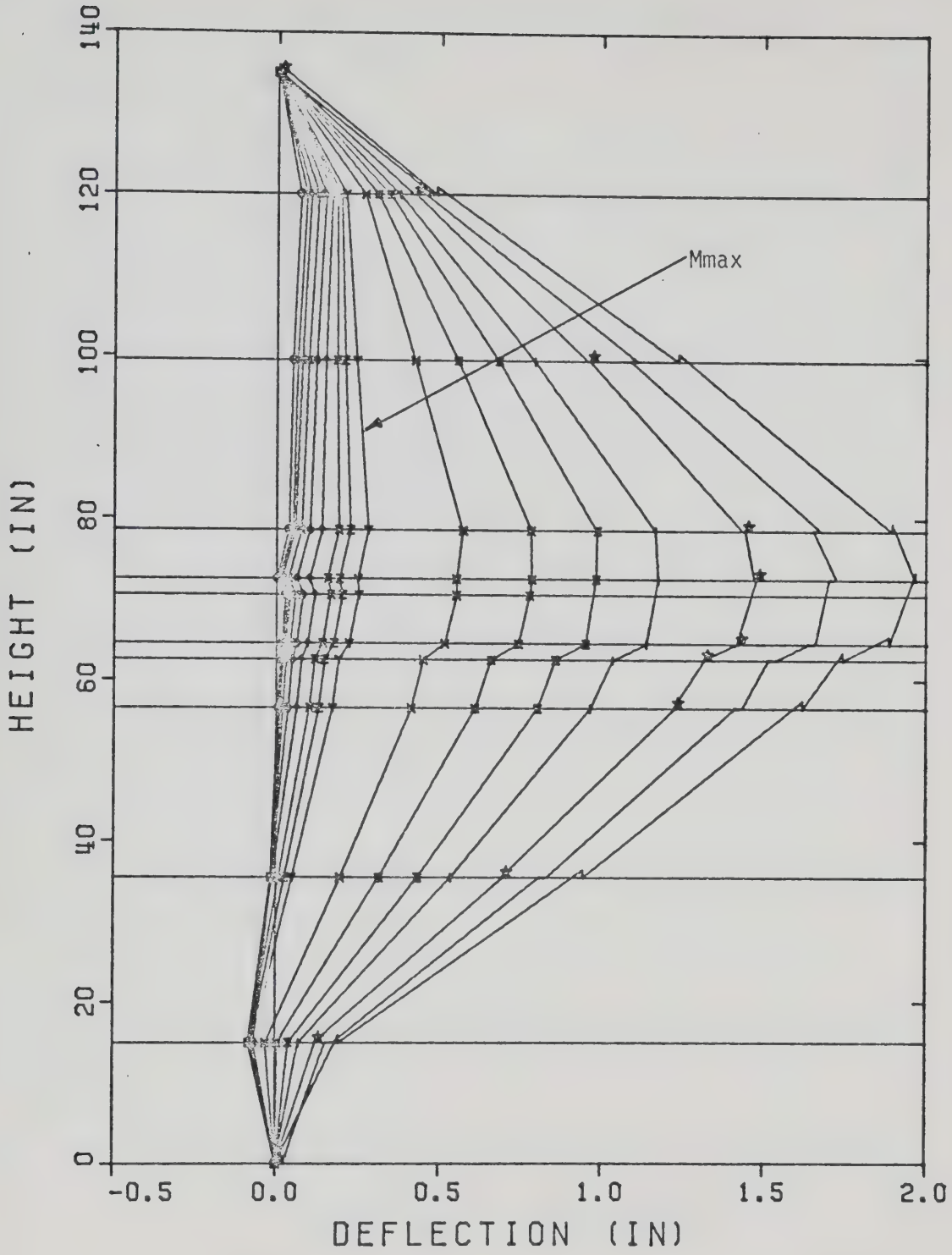

Fig. 4.8 Deflected Shape Of Wall B50

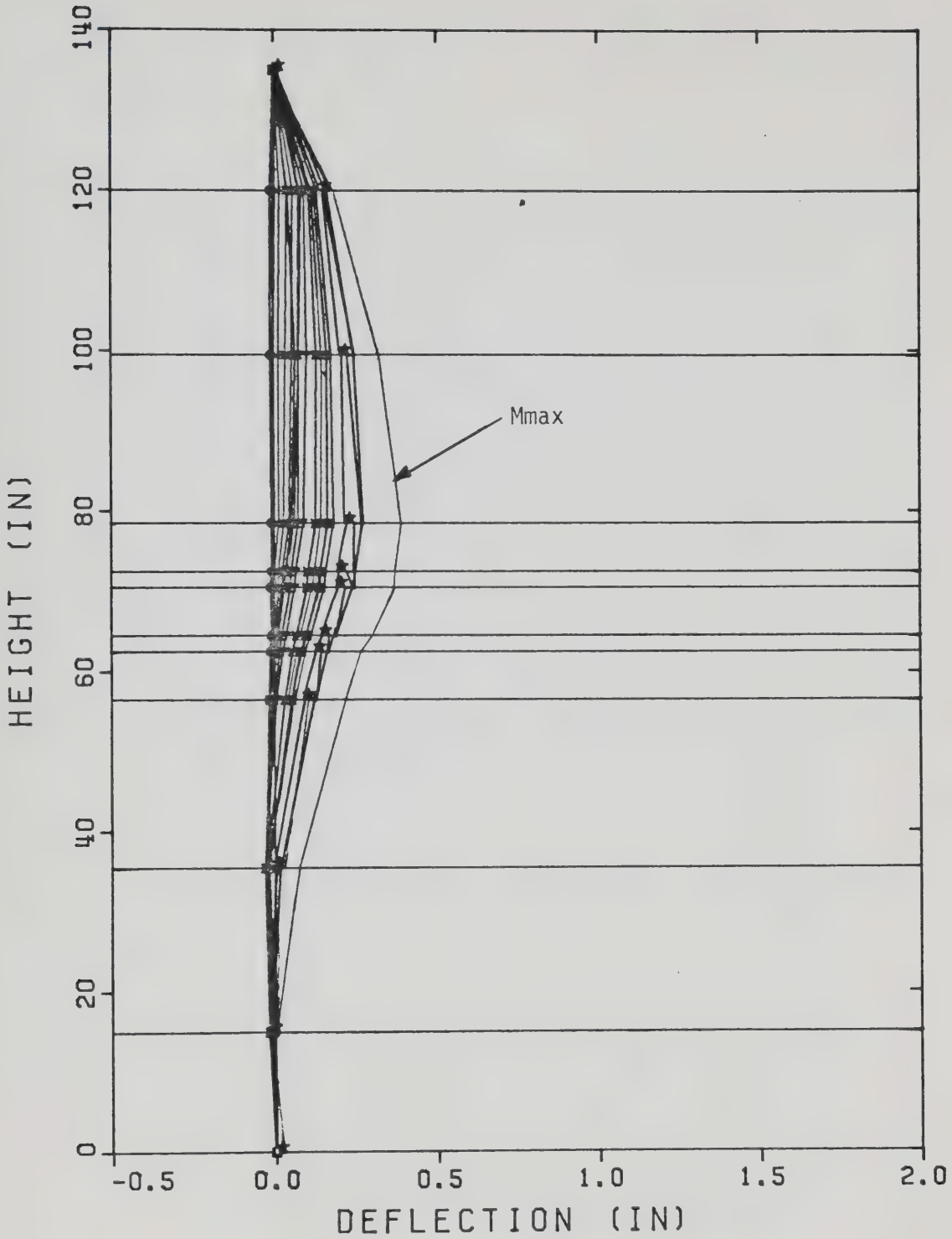

Fig. 4.9 Deflected Shape Of Wall B150

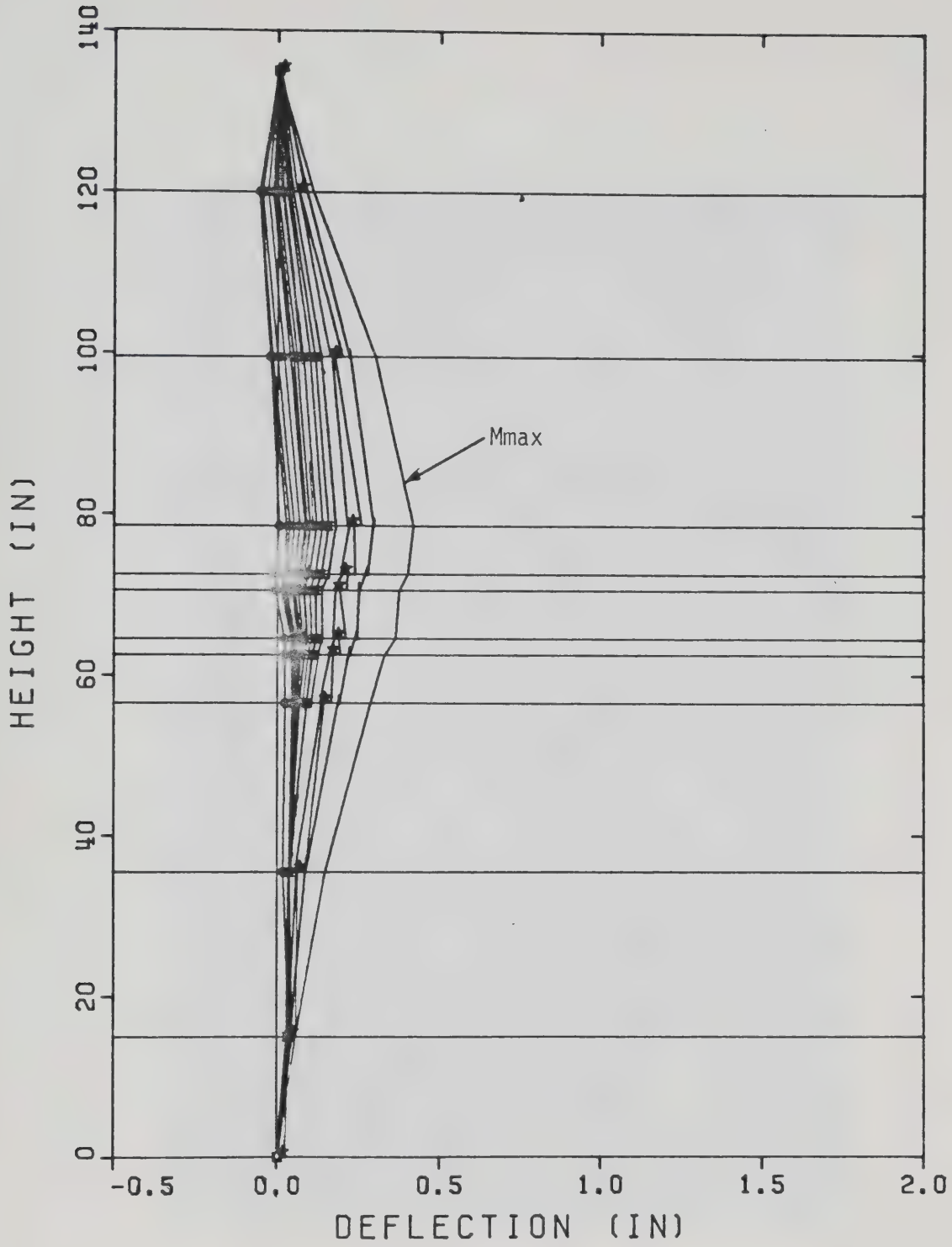

Fig. 4.10 Deflected Shape Of Wall B200

Plate 4.1 Wall A25 At Failure

Plate 4.2 Wall A100 At Failure

Plate 4.3 Wall B150 At Failure

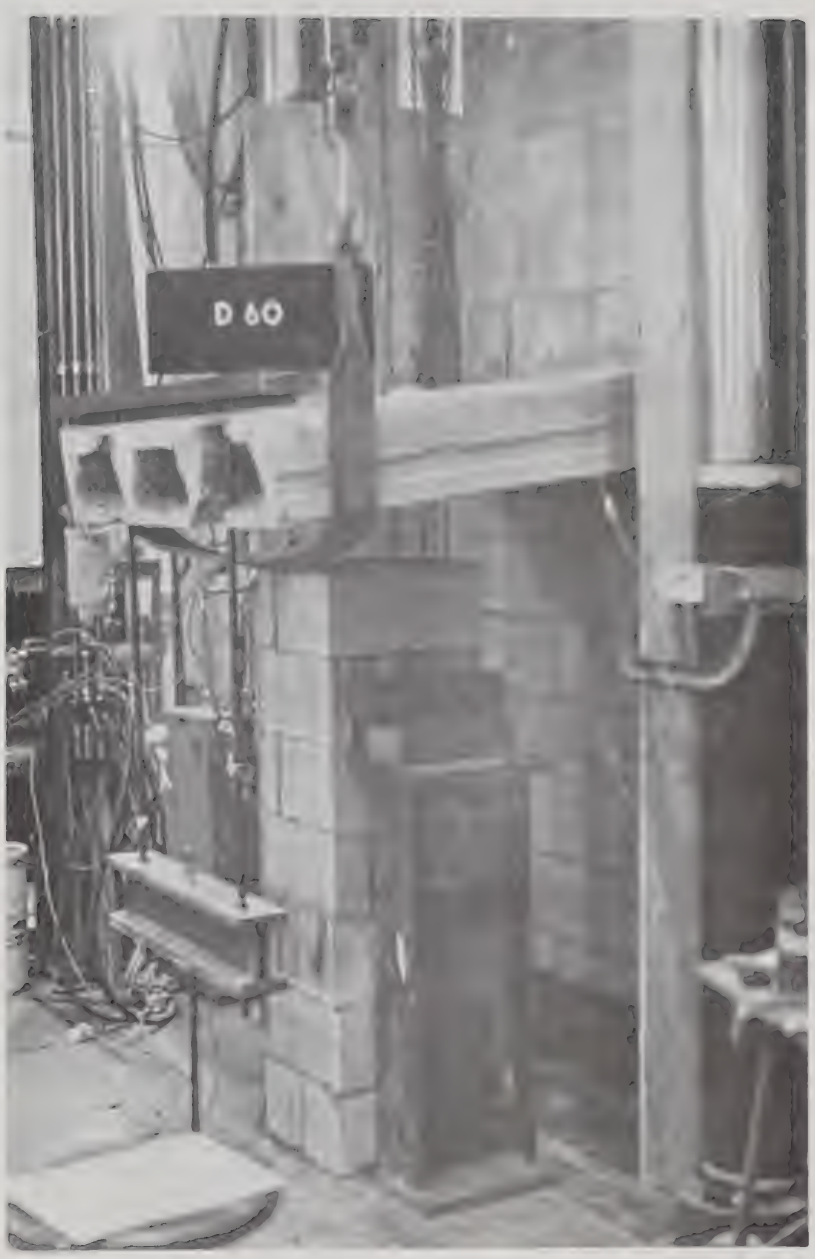

Plate 4.4 Wall D60 At Failure

5. Discussion of Test Results

5.1 Introduction

In this chapter, the experimental results are interpreted and compared with analytical results based on existing theories of concrete masonry strength and structural interaction.

The first section of this Chapter deals with specimens with cast-in-place slabs. The moment-rotation behavior, as it applies to the failure of the joint is compared with Sahlin's[1] theory of joint performance and analytical results based on theory presented by Hatzinikolas[10].

The second section deals with the performance of the specimens with precast slabs. The results are interpreted to explain the failure modes of these specimens.

Finally, the last section deals with the moment-rotation performance of the cast-in-place slabs while the joint remains rigid.

5.2 Failure of The Specimens With Cast-In-Place Slabs

5.2.1 Test Results Compared With Sahlin's Theory

In Chapter 2, a theory of wall-slab interaction by Sahlin was described. His explanation of the joint performance was that, upon applying a moment to the wall through a loaded floor slab, the rotation of the slab end (θh) is the same as the rotation of the wall end (θv), thus the wall-slab joint behaves rigidly. For all of the

specimens tested in the present investigation the joints were rigid up to the application of Mmax.

Failure category number one, where the joint remains rigid ($\emptyset = 0.$) and the wall fails due to eccentric loading, describes the compressive type failures of the test specimens. The walls in this case failed due to crushing of the concrete in the blocks immediately above the slab end. None of the specimens failed due to buckling.

In the second failure mode the walls and slab ends rotate rigidly ($\emptyset = 0.$) until a maximum moment, Mpl, is reached. At this point Sahlin states that the joint begins to rotate plastically ($\emptyset > 0.$) with a constant or decreasing moment being applied. This type of behavior occurred in the test specimens which had tension type failures.

Sahlin's third failure category describes the joint failing by reaching it's ultimate rotation capacity ($\emptyset = \emptyset ult$). The test specimens which had tension type failures did not exhibit this behavior. They had large horizontal deflections at the level of the slab and these deflections caused large P-Delta moments which altered the distribution of moments in the walls. Failure of the specimens occurred when the walls became unstable and tipped over.

5.2.2 Analytical Results of Joint Performance Based on Concrete Block Strength

Hatzinikolas developed a computer program, TPM, to predict theoretically the axial load-moment interaction

curve for eccentrically loaded concrete masonry walls. Curves are produced on the basis of the strength of the cross section, ($h/t = 0.$), and are later adjusted for slenderness, ($h/t > 0.$), by applying a moment magnifier. There was good correlation between the analytical results from the computer program and the results of tests of full scale wall specimens. The assumptions used in developing TPM along with a brief description of how the program works are presented in Appendix B. The interaction diagram and values of Mmax from the tests are plotted for unreinforced walls in Fig. 5.1 and for reinforced walls in Fig. 5.2.

A comparrison of the results of the wall-slab specimen tests with the results produced by TPM indicates that for a given level of axial load the value for Mmax was the same as the ultimate moment capacity of the wall. The joints of the specimens behaved rigidly until Mmax was reached, thus Mpl, at which Sahlin states that the joint begins to rotate plastically, is the same as Mmax. Mpl is the ultimate moment capacity corresponding to the level of axial load placed on the wall.

The behavior of the joint before Mmax is reached was typical of the behavior of an elastic material with no tensile strength. Section 5.4 deals with the moment distribution and joint rotation of the walls when the joint remains rigid.

For axial load values greater than Pb, the failure of the cross section is due to the stress at the compressive

edge of the wall reaching the maximum compressive strength of the block. Thus the test specimens which failed immediately upon reaching the maximum moment did so by crushing of the blocks. In the case of the the unreinforced walls the crushing was accompanied by splitting. Fig. 5.3 schematically depicts the stresses on a cross section of a wall having a compressive failure and Fig. 5.4 shows the stresses at failure when P = Pb.

For axial load values less than Pb, the cross section fails due to tensile cracking. The cracked or unloaded part of the cross section becomes so large that the internal stresses on the cross section cannot balance the applied loads. The compressive strength of the block is not reached and the joint is able to rotate with a decreasing moment. This performance may continue until the compressive strength of the block is reached. The rotation at which this occurs is defined by Sahlin as ϕ_{ult}. Fig. 5.5 depicts two cross sections of a wall with a tension failure having different internal stresses while being subjected to the same external axial load and moment.

The specimens did not exhibit the behavior of the wall end rotations remaining the same while the slab end rotations increased. The wall below the slab had a higher level of axial load than the wall above the slab. The part of the interaction curve for tension failures shows that a wall with higher axial load has a larger moment capacity. The upper wall then was cracked to a larger degree than the

lower wall, thus the lower wall had a higher moment of inertia. It is shown in Section 5.4 that the lower wall with the higher moment of inertia is stiffer or more resistant to rotation than the upper wall and that this stiffness caused the horizontal deflection at the slab level. The horizontal deflection in turn caused a P-Delta moment which increased the moment on the upper part of the wall while decreasing the moment on the lower wall. This cause-effect-cause behavior eventually becomes balanced with a large amount of the moment redistributed.

The horizontal deflection also altered the rotations of the ends of the walls. This along with the redistributed moments caused the stress distributions in the wall to be very complex making an accurate analysis difficult.

The walls and slabs in an actual building would not deflect in the same manner, therefore it would not be of much benefit to analyse the stress distribution after the large deflections have taken place. In further tests on joint performance it would be desirable to prevent the joint from deflecting horizontally. Such test specimens would better reflect the actual behavior of the wall-slab joints in a real building.

In conclusion, the wall-slab joints behaved rigidly until the moment capacity of the wall was reached. When the axial load on the wall was above Pb, the wall failed immediately upon reaching Mmax. When the axial load on the wall was below Pb, the joint began to rotate plastically

after Mpl was reached and the nature of the interaction of the walls and slabs was altered.

Although a method of analysis may be developed to predict the performance of the joint after Mpl is reached, interest in this performance is only academic. The joints no longer behave as rigid connections and attempting to design a structure accepting the plastic rotation of the joint is not advisable as the capacity of the wall has been exceeded. The large degree of cracking at the joint would not be acceptable in a real building and there is a danger of the walls becoming unstable.

5.3 Failure of Specimens With Precast Slabs

5.3.1 Joint Performance

The type of wall-slab connection used for the specimens with precast slabs was recommended by the manufacturer of the slabs to create a simply supported end condition. To achieve this the slab end must be able to rotate without rotating the wall ends and no moment must be developed at the slab end.

The test results indicate that there was very little interaction between the slabs and walls with this type of joint. The slab end rotated without rotating the wall ends because of the asbestos bearing pad placed under the slab. This pad was highly compressible and allowed the slab to drop at the face of the wall as the end rotated.

The part of the slab end behind the asbestos pad did have some interaction with the wall through the grout in the joint. Thus, a small amount of moment was developed and transferred to the walls. The slab could be considered fixed behind the asbestos pad. Moment was developed in the slab until the tensile strength of the grout was reached and a tensile crack appeared at the slab end. Continued rotation of the slab end caused both the width and depth of the crack to increase.

The moment in the specimens with wrap-around bars did not drop significantly because the bars acted as tension reinforcement. The moment in the slabs without the wrap-around bars dropped very quickly after the tensile crack appeared. As expected, the wrap-around bars also prevented the slab from pulling or rotating out of the joint by bearing against the vertical reinforcement.

A simply supported slab with the same stiffness as those used in the tests, spanning 20 feet and subjected to normal occupancy loads, would have an end rotation of approximately 2-3/4 degrees. The slabs of the test specimens were rotated more than this amount without causing failure of the wall if the wall was not subjected to a large axial load. The problems associated with large axial loads will be discussed later.

Therefore, the joint detail can be assumed to provide a simply supported end condition for the slabs, and the walls can be assumed to have almost no eccentricity of load.

5.3.2 Effect of the Precast Slab Joint on Masonry Wall Performance

The theory of failure of axially loaded concrete masonry walls is well documented and accepted. Concrete blocks and mortar each possess a different Poissons ratio. Because of this, the mortar, when loaded, expands in the unconfined direction more than the concrete blocks. The blocks, through shear stresses, attempt to confine the mortar, thus tensile stresses are produced in the blocks. Eventually the tensile stresses exceed the tensile strength of the blocks and splitting cracks appear. Increasing the axial load on the wall causes the tensile cracks to grow larger and eventually results in failure of the wall by vertical splitting.

As stated before, the joint detail used for the precast slabs allowed the slab end to rotate and this caused a vertical crack to be initiated at the precast slab end. This crack appears at the same location as the tensile splitting crack would appear in an axially loaded wall. The early initiation of the crack lowered the axial load capacity of the wall.

Also, because the asbestos pad was so compressible, the effective elastic modulus on the side of the wall with the pad was much lower than the side without the pad. Therefore, most of the load applied to the wall was transferred through the joint onto the part of the wall without the pad. The stresses then were higher there than

in other levels of the wall.

Wall E350 was subjected to axial load only and no vertical cracks were present at the time of loading. Eventually a vertical crack appeared behind the slab end. The wall failed under a much lower load than similar walls tested by Hatzinikolas. The early initiation of the splitting crack was due to three factors:

a. The compressive stresses were higher at the joint.

b. The asbestos pad allowed its side of the wall to vertically deflect more than the other side, thus vertical shear stresses were present at the end of the slab.

c. The tensile strength of the grout-slab bond is less than the tensile strength of a block which would normally be at this position.

All of the specimens on which the axial load was increased to failure after the crack was initiated failed by vertical splitting at much lower loads than would normally be expected.

Hatzinikolas subjected walls, similar to the walls used in the present test specimens, to axial loads. He found that the average stress at failure, based on the net bedded area of the mortar, was 1700 psi. The unreinforced specimens of this test series failed at a load of 120 to 140 kips. Based on the net area, this would yield a stress of 910 to 1060 psi; stresses much lower than those of Hatzinikolas' tests. If computed on the net bedded area of

the wall not bearing on the asbestos pad, the stress is found to be between 1700 to 2000 psi.

When using this type of joint detail the designer should be aware of the effect that the joint has on the axial load capacity of the walls. It is advisable to consider only the net area of the wall behind the asbestos pad for strength calculations.

5.4 Moment-Rotation Analysis of Specimens With a Rigid Joint

5.4.1 Structural Analysis of a Rigid Frame

In the design of members for a frame structure the designer must first predict the loads and moments on the members. Building codes give detailed guidelines on choosing the amount of wind, occupancy and other loads.

Methods to find the distribution of moments on the members of a rigid frame have been developed and are widely used for structural materials such as steel and concrete. If concrete masonry walls are found to behave in a predictable manner then it is logical to assume that their interaction with other members in a frame structure can also be analysed. The steps required to carry out a structural analysis are as follows:

a. Determine all of the loading conditions on the structure.

b. Pick trial members and estimate the values for Em and Ie.

c. Complete a rigid frame analysis using any of the

accepted methods

d. Check that the capacity of the trial members has not been exceeded and check the estimate of Em and Ie.

e. If the trial members and the estimates for Em and Ie are acceptable the process is over. If not, the process must be redone starting from step (b). If the load-moment capacity of the wall has been exceeded, the joint will no longer act rigidly. Therfore the trial section picked for the wall is insufficient and a new section will have to be used.

5.4.2 Test Specimens Modeled For a Rigid Frame Analysis

The amount of moment developed on a member framing into a rigid joint is a fraction of the total moment placed on the joint. It is proportional to the amount of resistance to rotation the member has to the total resistance to rotation of all of the members framing into the joint.

The slabs of the test specimens were cantilevered and were loaded so as to rotate their ends, thus producing the moment on the wall-slab joint. As the slab end rotates the ends of the walls must rotate an equal amount if the joint is to remain rigid. The walls resist end rotation to a degree dependent on their stiffness and the applied slab moment is proportionally resisted by them.

While the slopes of the applied moment-slab end rotation plots presented in Chapter 4 are not linear they are all similar up to a moment equal to Mmax. Beyond Mmax the joint did not act as a rigid connection between the

walls and slab.

As the axial loads placed on the wall increased the slope of the moment-rotation plot also increased. Thus the wall-slab joints of the specimens subjected to higher axial loads were more resistant to rotation than those of specimens subjected to lower loads. This indicates that walls subjected to higher axial loads have a higher stiffness than those subjected to lower axial loads.

The resistance to rotation or stiffness of the wall is a function of the elastic modulus, Em, the material in the wall and the moment of inertia, I, of the cross section of the wall. As any of these quantities increase so does the stiffness of the wall.

The elastic modulus of concrete masonry has not been intensively researched. Generally, as the axial load on the wall increases so does Em, also the value for Em is not the same for unloading as it is for loading. CSA S304 1977 recommends that Em be estimated as 1000f'm and Hatzinikolas has recommended that this value be lowered to 750f'm. Because the materials used in this study are the same as those used by Hatzinikolas the value of 750f'm was used for this analysis. This yields a value for Em of 1300 ksi.

The moment of inertia of the walls varies along their height due to tensile cracking. An equivalent moment of inertia, Ie, for the whole wall is required to estimate the stiffness of the wall. Hatzinikolas developed an equation for the equivalent stiffness of an unreinforced wall to be

used for design calculations. The equation is:

$$Ie = 2*(1/2 - e/t)*Io$$

Where Io = Moment of inertia of the uncracked section.

This equation represents a straight line plot of Ie vs e/t with intercepts at Ie =Io (when e/t = 0.) and Ie =0. (when e/t =1/2). For small values of e/t this relation was found to yield satisfactory results for Ie when compared to results from both this test series and Hatzinikolas' tests. However, for larger values of e/t the equation greatly underestimates Ie. This may be conservative for design calculations but the value of Ie must be more accurately determined when it is used for the analysis of a structure. The plot of Ie vs e/t presented by Hatzinikolas indicates that a 2nd degree parabola may more accurately describe the relationship.

At the present time there is no satisfactory method for predicting the value of Ie for cracked concrete masonry walls subjected to large moments. Obviously the value of Ie must be a fraction of the uncracked moment of inertia, Io.

It is logical to assume that a wall subjected to a higher axial load will have less cracking than a wall subjected to a lower load when both are subjected to the same moment. Thus the more highly loaded wall will have a higher value for Ie and therefore greater stiffness. This assumption is supported by the test results.

To try and predict the rotation and deflection behavior of the specimens, a computer program, PFT, was used. This

program is a modified version of the "Plane Frame and Truss Program" [13] and is one of the programs currently used at the University of Alberta for the structural analysis of rigid frames. The assumptions of material behavior in the program are widely accepted and used in most structural analysis methods. The program computes end moments, end shears and end axial forces for each member in a plane frame and computes horizontal deflections, vertical deflections and rotations of each joint.

The specimens were modeled by placing joints at the location of the two pinned ends of the walls, the wall-slab joint and fixed joints were placed at the level of transducers 2 and 9. The output included the rotation of the wall end and slab end and the deflections of all of the joints.

The elastic modulus of the concrete slab, Ec, computed according to the privisions of Section 8.5.1 of ACI 318-77, was 3600 ksi. The moment of inertia of the concrete slab, computed as the cracked section moment of inertia, Icr, was 811 in^4. As previously stated Em was taken as 1300 ksi.

The program computes the deflections of the joints but it does not compute the P-Delta moments which are associated with these deflections. To overcome this deficiency the locations of the joints were read into the program at their deflected positions.

5.4.3 Comparison of Test Results With Results of a Rigid Frame Analysis

The purpose of this section is to determine if the test specimens behaved in a predictable manner and to determine if the wall-slab joint behaved rigidly up to Mmax.

If all the data read into PFT accurately represented the actual values for Em and Ie of the test specimens then the results from PFT should compare favorably with those actually measured on the test specimens. The major variables were the values for the moment of inertia, Ie, of the walls above and below the slab. A trial and error procedure was used to determine these values.

In general, it was found that the deflections of all of the joints and the rotations of the slab end could be successfully predicted by PFT after a few iterations. Tables 5.1, 5.2, and 5.3 show the values predicted by PFT and those actually measured for specimens A50, B25, and B50.

The wall stiffness for specimens with small amounts of applied slab moment was close to Io and as the moment increased the values for Ie decreased. As the walls were subjected to higher axial loads the value of Ie for a given level of moment was generally higher. Exceptions to this were found in specimens where the deflections or axial loads were very high and the associated P-Delta moments caused large deviations from normal.

In order that the wall-slab joint deflect horizontally in the same direction as in the test specimen the bottom

wall had to be modeled stiffer (with a higher Ie) than the top wall. This agrees with the supposition that the walls subjected to higher axial loads and smaller moments, as the bottom walls were, have less cracking and therefore a higher Ie.

There did not seem to be any exact correlation between the levels of axial load and moment on the wall and the value for Ie. The largest discrepancies occurred in the specimens with high P-Delta moments. Because there is a large degree of indeterminancy associated with the P-Delta moments, it would be advantageous in further tests to prevent the specimens from deflecting horizontally at the level of the slab. by doing so, many of the unknown factors would be removed and the specimen could be modeled in a more exact manner. Then the values for Ie for the top and bottom walls may be found to have a meaningful correlation with the level of axial load and moment placed on the specimen.

The statics of masonry wall-floor slab interaction have been solved using the computer program PFT. Although the results were produced by a trial and error procedure, once more research has been conducted and a successful method of predicting Em and Ie has been found, the structural analysis of statically indeterminate frames with concrete masonry bearing walls could be undertaken as it is with concrete and steel.

Table 5.1 Computed and Measured Rotations and Deflections for Specimen A50

Incr	Msl	Ie		θh	Horizontal Deflection in Transducer #			
		Upper	Lower					
	kip-in	in^4	in^4	degrees	2	5	9	
6	179.	800.	1300.	.09	.060	.070	.020	c
				.08	.113	.080	.040	m
8	259.	800.	1200.	.15	.115	.108	.040	c
				.11	.146	.105	.050	m
10	323.	700.	1100.	.23	.201	.225	.103	c
				.24	.238	.235	.102	m
12	308.	700.	1100.	.25	.383	.499	.282	c
				.37	.387	.529	.248	m

1. c = computed values
2. m = measured values

Table 5.2 Computed and Measured Rotations and Deflections for Specimen B25

Incr	Msl	Ie		θh	Horizontal Deflection in Transducer #			
		Upper	Lower					
	kip-in	in^4	in^4	degrees	2	5	9	
7	161.	1400.	1800.	.05	.017	.012	.000	c
				.03	.019	.030	.015	m
9	212.	1300.	1250.	.11	.109	.133	.050	c
				.09	.062	.080	.036	m
11	270.	1050.	1100.	.17	.170	.208	.090	c
				.23	.161	.210	.091	m
12	278.	850.	1000.	.21	.226	.282	.129	c
				.26	.203	.275	.125	m
13	267.	550.	850.	.34	.419	.534	.265	c
				.37	.333	.500	.241	m

1. c = computed values
2. m = measured values

Table 5.3 Computed and Measured Rotations and Deflections for Specimen B50

Incr	Msl	Ie		θh	Horizontal Deflection in Transducer #			
		Upper	Lower					
	kip-in	in^4	in^4	degrees	2	5	9	
3	79.	800.	1300.	.03	.015	.013	.000	c
				.06	.031	.011	.016	m
5	151.	700.	750.	.11	.045	.030	.004	c
				.11	.061	.030	.000	m
7	261.	700.	500.	.19	.075	.052	.000	c
				.16	.095	.050	.000	m
9	358.	700.	750.	.26	.124	.102	.011	c
				.26	.147	.102	.014	m
11	402.	650.	650.	.32	.191	.182	.050	c
				.37	.206	.180	.023	m
13	443.	650.	650.	.32	.421	.530	.275	c
				.36	.421	.530	.195	m

1. c = computed values
2. m = measured values

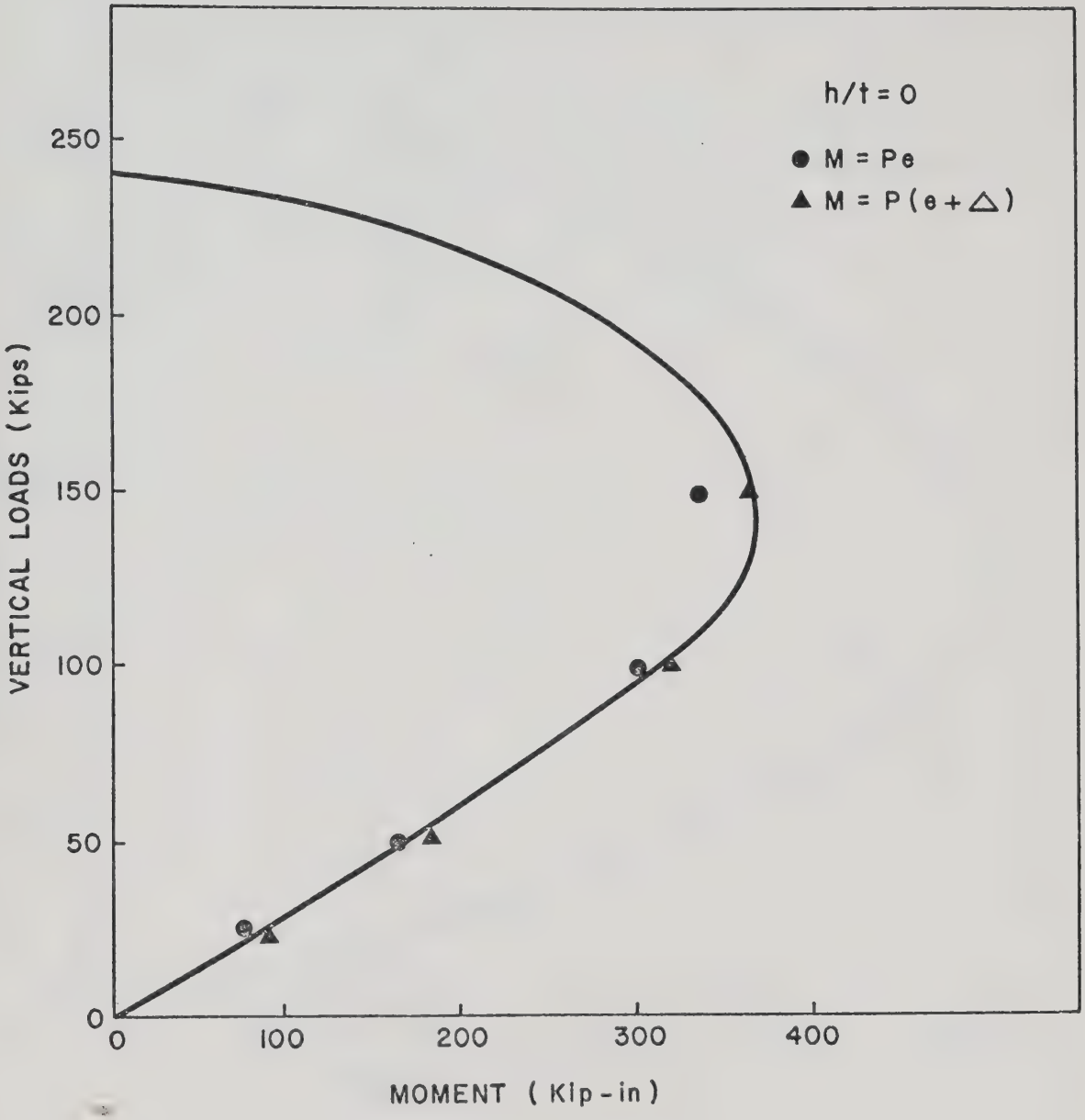

Fig. 5.1 Moment Interaction Diagram for Unreinforced Walls

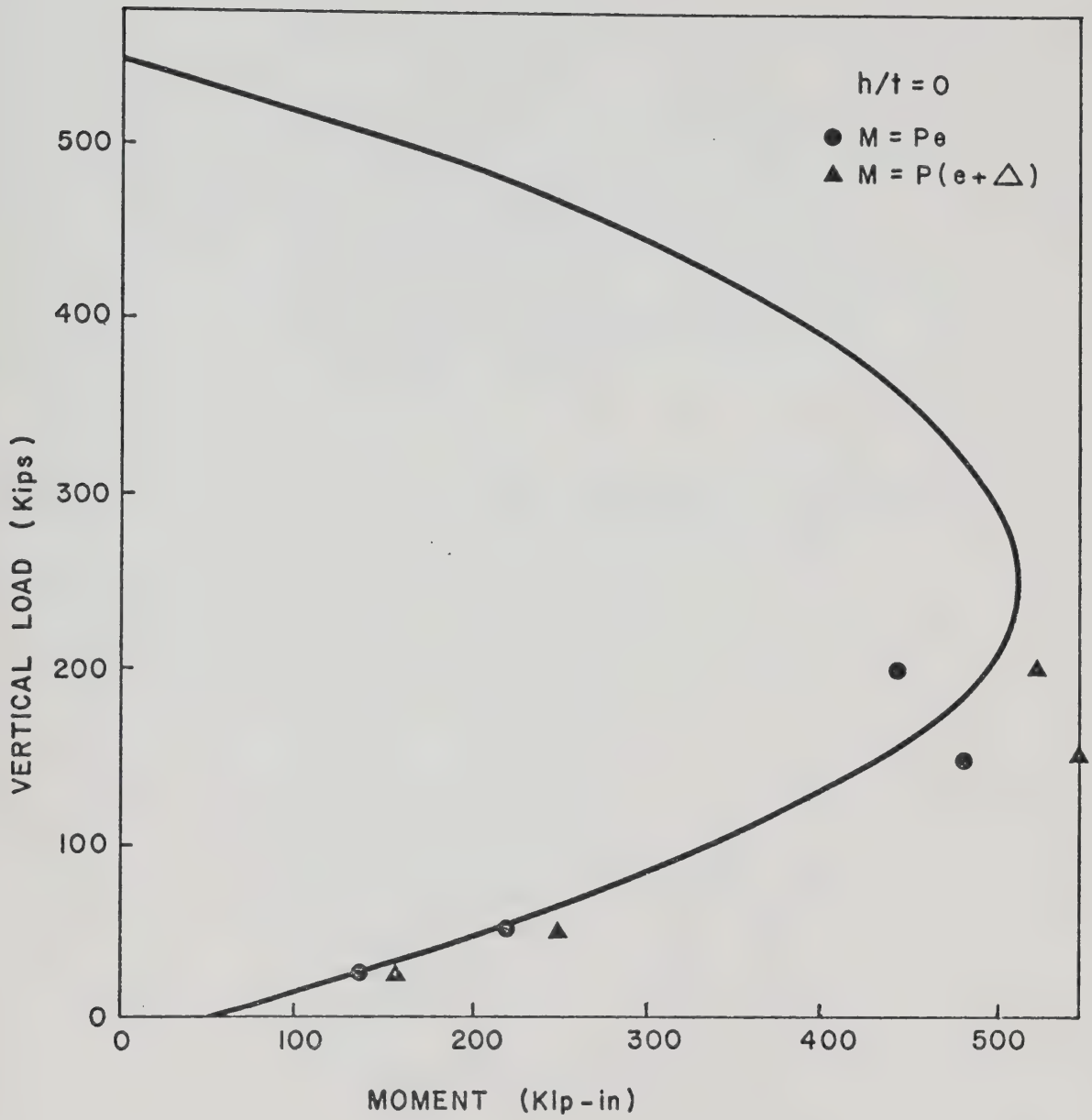

Fig. 5.2 Moment Interaction Diagram for Reinforced Walls

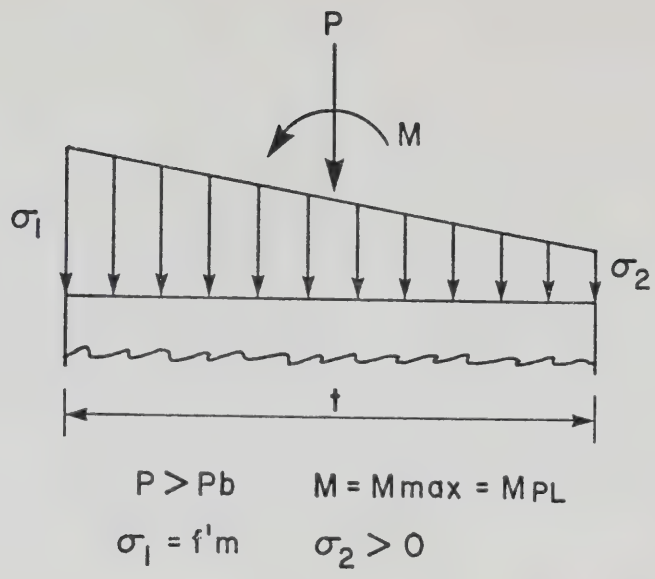

Fig. 5.3 Internal Stress Distribution on a Wall Cross Section Having A Compressive Failure

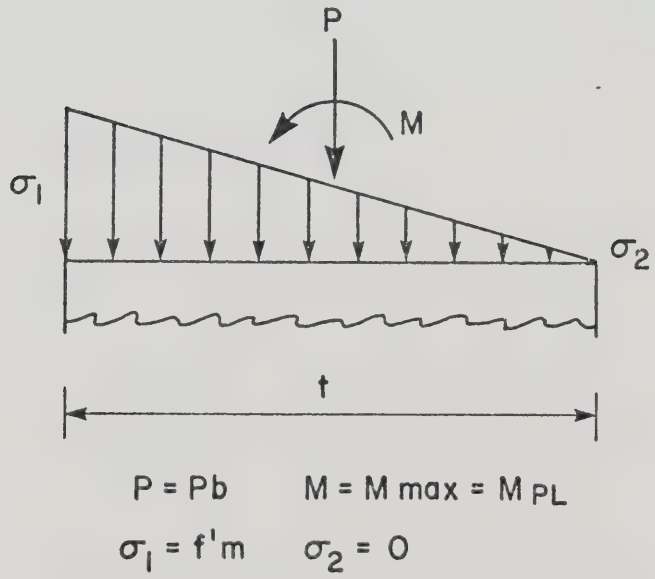

Fig. 5.4 Internal Stress Distribution on a Wall Cross Section Having a Balanced Failure

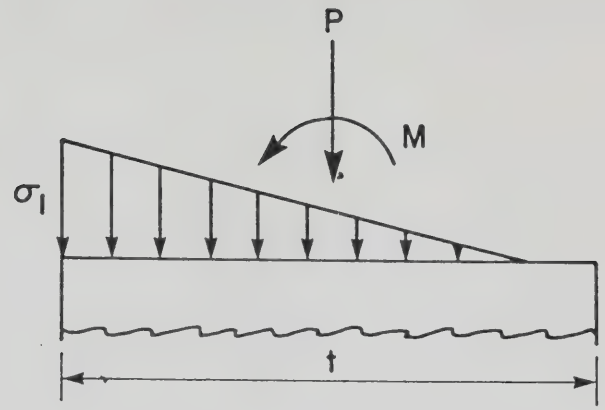

$P < Pb \qquad M = M\,max. = M_{PL}$

$\sigma_1 < f'm \qquad \phi = 0$

A) Stresses When M=Mpl and Ø=0.

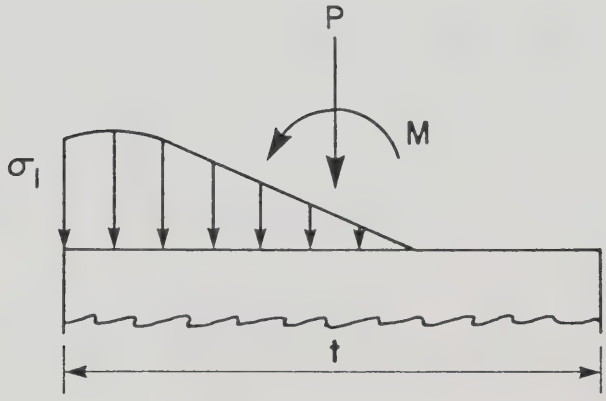

$P < Pb \qquad M = M\,max = M_{PL}$

$\sigma_1 = f'm \qquad \phi = \phi_{ULT}$

B) Stresses When M=Mpl and Ø=Øult

Fig. 5.5 Internal Stresses Distribution on a Wall Having a Tension Failure

6. Summary, Conclusions and Recommendations

6.1 Summary

This investigation was undertaken to examine the behavior of the joint between a concrete masonry bearing wall and a loaded floor slab. The experimental phase of the study consisted of tests on full scale wall-slab combinations, with both cast-in-place and precast concrete slabs. The purpose of the tests was to examine the effect of the magnitude of axial wall load on the failure mode and slab end rotation for specimens with various joint details. The analytical phase of the study included evaluation of the strength characteristics of the masonry walls and analysis of the specimens as rigid frames. The test results were compared with the analytical results and existing theories of joint performance.

6.2 Observations and Conclusions

The conclusions of this study are:

a. The joint detail used for the specimens with precast slabs allowed significant slab end rotations with small moments. This detail can be assumed to provide a simply supported end condition for the precast slabs.

b. The joint detail used for the specimens with precast slabs reduced the load carrying capacity of the masonry walls significantly.

c. The behavior of the eight test specimens with cast-in-place slabs was similar to the behavior described by Sahlin[2].

d. Although, in some cases, the specimens with cast-in-place slabs remained stable after Mmax was reached and further end rotations could be induced, the nature of the interaction of the walls and slabs was altered. Sufficient cracking of the concrete around the slab had occurred to conclude that the joint had reached its useful limit. Thus, the failure of the specimens occurred when the ultimate moment capacity of the masonry walls was reached.

e. The joint of the specimens with cast-in-place slabs can be considered as a rigid connection between the walls and slabs until the ultimate moment capacity of the walls is reached.

f. The degree of fixity of the rigid joint of the specimens with cast-in-place concrete slabs is a function of the stiffness of the masonry walls, as the stiffness of the walls increased so did the resistance to rotation of the slab end. This stiffness, dependent on the equivalent moment of inertia and modulus of elasticity of the cracked wall, decreased as the level of axial load on the wall decreased and as the moment transferred to the wall increased, due to cracking of the wall.

g. Structural analysis of a structure consisting of

loadbearing masonry walls and cast-in-place concrete slabs with joint details like those used in this study can be evaluated using existing rigid frame analysis methods.

6.3 Recommendations

The recommendations from this study are:

a. When using the type of joint detail of the specimens with precast slabs the designer should consider only the net area behind the asbestos pad for calculations of the wall strength.

b. Research should be carried out to evaluate the modulus of elasticity and the effective moment of inertia for a cracked wall subjected to flexural stresses. Special attention should be paid to developing a theoretical relationship between the level of axial load and moment on the wall to the stiffness of the wall.

c. Further tests on wall-slab interaction specimens should be undertaken. The specimens should be similar to the cast-in-place slab specimens used in this series but with lateral restraint at the floor levels. The investigation should consider tests on differring rigid joints with special attention paid to developing a method of rigid frame analysis for the test specimens and eventually a real structure.

References

1. Sahlin, S. "Structural Interaction of Walls and Floor Slabs." National Swedish Council for Building Research, Report No. 35, 1959.

2. Sahlin, S. "Interaction of Brick Masonry Walls and Concrete Slabs." Designing, Engineering and Constructing with Masonry Products, Ed. F.B. Johnson. Houston, Gulf Publishing Co., 1969.

3. Sahlin, S. "Structural Masonry." Englewood Cliffs, N.J., Prentice Hall, 1971.

4. Maurenbrecher, A.H.P., and Hendry, A.W. "Aspects of the Strength and Fixity of the Joint Between a Brick Wall and a Floor Slab." Proceedings of the 2nd International Brick Masonry Conference, Stoke-on-Trent, April, 1970.

5. Colville, J., and Hendry, A.W. "Aspects of A Load Bearing Masonry Structure." 6th International Symposium on Load Bearing Brickwork, London, 1977.

6. Risager, S. "Structural Behavior of Linear Elastic Walls Having No Tensile Strength." Designing, Engineering and Constructing With Masonry Products. Ed. F.B. Johnson. Houston, Gulf Publishing Co., 1969.

7. Sinha, B.P., and Hendry, A.W. "An Investigation into the Behavior of a Brick Cross-Wall Structure." 6th Internation Symposium on Load Bearing Brickwork, London, 1977.

8. Furler, R., and Thurliman, B. "Strength of Brick Walls Under Enforced End Rotations." 6th International

Symposium on Load Bearing Brickwork, London, 1977.

9. Germanino, G., and Macchi, G. "Experimental Research of a Frame-Idealization for a Bearing Wall Multistory Structure." 6th International Symposium on Load Bearing Brickwork, London, 1977.

10. Hatzinikolas, M. "Concrete Masonry Walls." Ph.d. Thesis, University of Alberta, Edmonton, Fall, 1978.

11. "Recommended Practice for Engineered Brick Masonry." Structural Clay Products Institute, August, 1969.

12. "A Design Guide to the Engineered Clay Masonry Bearing Wall System." Clay Brick Association of Canada, BCI 5.4 Division 4, Willowdale, Ontario, 1975.

13. Beaufait, F.W., Rowan, W.L., Hoadly, P.G., and Hackett, R.N. "Computer Methods of Structural Analysis." Englewood Cliffs, N.J., Prentice Hall, 1970.

14. Hognestad, E. "A Study of Combined Bending and Axial Load in Reinforced Concrete Members." University of Illinois, Engineering Experimental Station, Bullitin Series No. 399, November 1951, 128 pp.

A. Calculated Results for Specimens With Precast Slabs

This appendix contains the moment versus slab rotation relationships for all of the specimens with precast slabs. The data is presented in both graphic and in tabular form.

Table A.1 Moments and Rotations For Wall C60

Incr No.	Mslab Kip-In	Mu Kip-In	θvl Degrees	θh Degrees	θvu Degrees	θhdef Degrees
4	16.	8.	0.04	0.12	-0.04	0.03
5	114.	57.	0.04	0.15	0.0	0.09
6	170.	85.	0.03	0.16	0.03	0.14
7	60.	30.	0.03	0.06	-0.01	0.41
8	47.	24.	0.02	0.06	-0.01	0.72
9	39.	19.	0.02	0.06	-0.02	1.12
10	37.	18.	0.02	0.06	-0.02	1.47
11	40.	20.	0.01	0.07	-0.02	2.24
12	36.	18.	0.01	0.07	-0.01	2.97
13	0.	-0.	0.00	0.04	-0.01	3.84
14	0.	-0.	0.00	0.04	-0.02	3.96

Table A.2 Moments and Rotations For Wall D60

Incr No.	Mslab Kip-In	Mu Kip-In	θvl Degrees	θh Degrees	θvu Degrees	θhdef Degrees
3	30.	15.	0.12	0.10	0.14	0.18
4	98.	50.	0.16	0.18	0.18	0.22
5	119.	61.	0.18	0.21	0.19	0.24
6	144.	73.	0.19	0.21	0.21	0.26
7	165.	85.	0.21	0.23	0.22	0.29
8	139.	72.	0.23	0.24	0.23	0.43
10	130.	68.	0.24	0.23	0.22	0.76
11	135.	71.	0.25	0.25	0.23	0.93
13	140.	74.	0.26	0.27	0.24	1.27
15	145.	77.	0.28	0.29	0.25	1.93
18	142.	76.	0.25	0.29	0.26	3.13
19	139.	74.	0.22	0.23	0.26	3.57
21	130.	69.	0.20	0.20	0.26	4.40
23	121.	64.	0.18	0.16	0.25	5.35
24	119.	63.	0.18	0.18	0.23	5.76
26	112.	59.	0.21	0.20	0.24	6.62
28	108.	58.	0.24	0.25	0.24	7.35
31	102.	55.	0.25	0.25	0.26	8.68
33	84.	45.	0.17	0.16	0.25	9.56

Table A.3 Moments and Rotations For Wall D120

Incr No.	Mslab Kip-In	Mu Kip-In	θvl Degrees	θh Degrees	θvu Degrees	θhdef Degrees
7	56.	32.	0.10	0.03	0.09	0.14
8	85.	47.	0.11	0.03	0.10	0.16
9	100.	55.	0.11	0.03	0.11	0.17
10	128.	69.	0.11	0.04	0.11	0.19
11	148.	79.	0.11	0.06	0.13	0.20
12	165.	87.	0.11	0.06	0.14	0.22
13	190.	100.	0.11	0.06	0.14	0.26
14	154.	82.	0.11	0.07	0.14	0.37
15	138.	74.	0.10	0.09	0.14	0.51
16	136.	73.	0.10	0.09	0.16	0.68
17	134.	72.	0.10	0.09	0.16	0.84
18	134.	72.	0.10	0.08	0.16	1.02
19	135.	72.	0.10	0.08	0.16	1.16
20	136.	73.	0.09	0.09	0.16	1.59
21	129.	68.	0.03	0.10	0.18	2.03
22	130.	68.	0.01	0.10	0.18	2.40
23	119.	61.	0.01	0.08	0.12	2.79
25	114.	55.	-0.01	0.06	0.08	3.63
26	109.	47.	-0.03	0.03	-0.03	3.97

Table A.4 Moments and Rotations For Wall E60

Incr No.	Mslab Kip-In	Mu Kip-In	θvl Degrees	θh Degrees	θvu Degrees	θhdef Degrees
4	30.	17.	0.02	0.04	0.02	0.04
5	58.	31.	0.02	0.05	0.04	0.06
6	78.	41.	0.03	0.07	0.03	0.07
7	112.	58.	0.04	0.07	0.06	0.09
8	133.	69.	0.04	0.08	0.06	0.11
9	147.	76.	0.05	0.09	0.06	0.12
10	173.	89.	0.06	0.10	0.08	0.15
11	187.	97.	0.07	0.12	0.08	0.20
12	192.	100.	0.08	0.14	0.08	0.28
13	164.	87.	0.09	0.14	0.08	0.41
14	151.	82.	0.12	0.17	0.08	0.64
15	142.	82.	0.17	0.22	0.11	1.15
18	134.	83.	0.23	0.30	0.30	2.27
20	128.	81.	0.27	0.34	0.40	3.06
21	124.	80.	0.26	0.34	0.43	3.53
24	100.	62.	0.17	0.24	0.39	4.69
25	96.	57.	0.13	0.18	0.32	5.15
26	90.	52.	0.10	0.15	0.30	5.62
29	80.	29.	-0.16	-0.22	0.08	7.25

Table A.5 Moments and Rotations For Wall E120

Incr No.	Mslab Kip-In	Mu Kip-In	θvl Degrees	θh Degrees	θvu Degrees	θhdef Degrees
4	30.	8.	-0.09	-0.02	-0.02	-0.08
5	79.	32.	-0.09	-0.02	0.00	-0.07
6	104.	45.	-0.07	-0.02	-0.00	-0.05
7	126.	55.	-0.07	-0.02	-0.00	-0.04
8	150.	68.	-0.07	-0.02	-0.00	-0.02
9	174.	80.	-0.07	-0.02	-0.00	-0.00
10	183.	84.	-0.07	0.01	-0.00	0.02
11	191.	88.	-0.07	0.03	-0.00	0.04
12	149.	66.	-0.09	0.01	0.05	0.19
13	113.	44.	-0.12	-0.03	0.02	0.71

Table A.6 Moments and Rotations For Wall E250

Incr No.	Mslab Kip-In	Mu Kip-In	θvl Degrees	θh Degrees	θvu Degrees	θhdef Degrees
8	30.	5.	-0.06	0.05	0.26	0.15
9	41.	8.	-0.06	0.05	0.27	0.16
10	55.	15.	-0.06	0.06	0.28	0.18
11	80.	27.	-0.06	0.06	0.29	0.20
12	89.	30.	-0.06	0.06	0.29	0.22
13	97.	33.	-0.07	0.06	0.30	0.25
14	91.	21.	-0.10	0.03	0.33	0.38
15	60.	-13.	-0.16	-0.06	0.32	0.64
16	54.	-26.	-0.21	-0.10	0.32	0.80
17	50.	-39.	-0.28	-0.14	0.32	0.96
18	6.	-76.	-0.34	-0.21	0.33	1.14

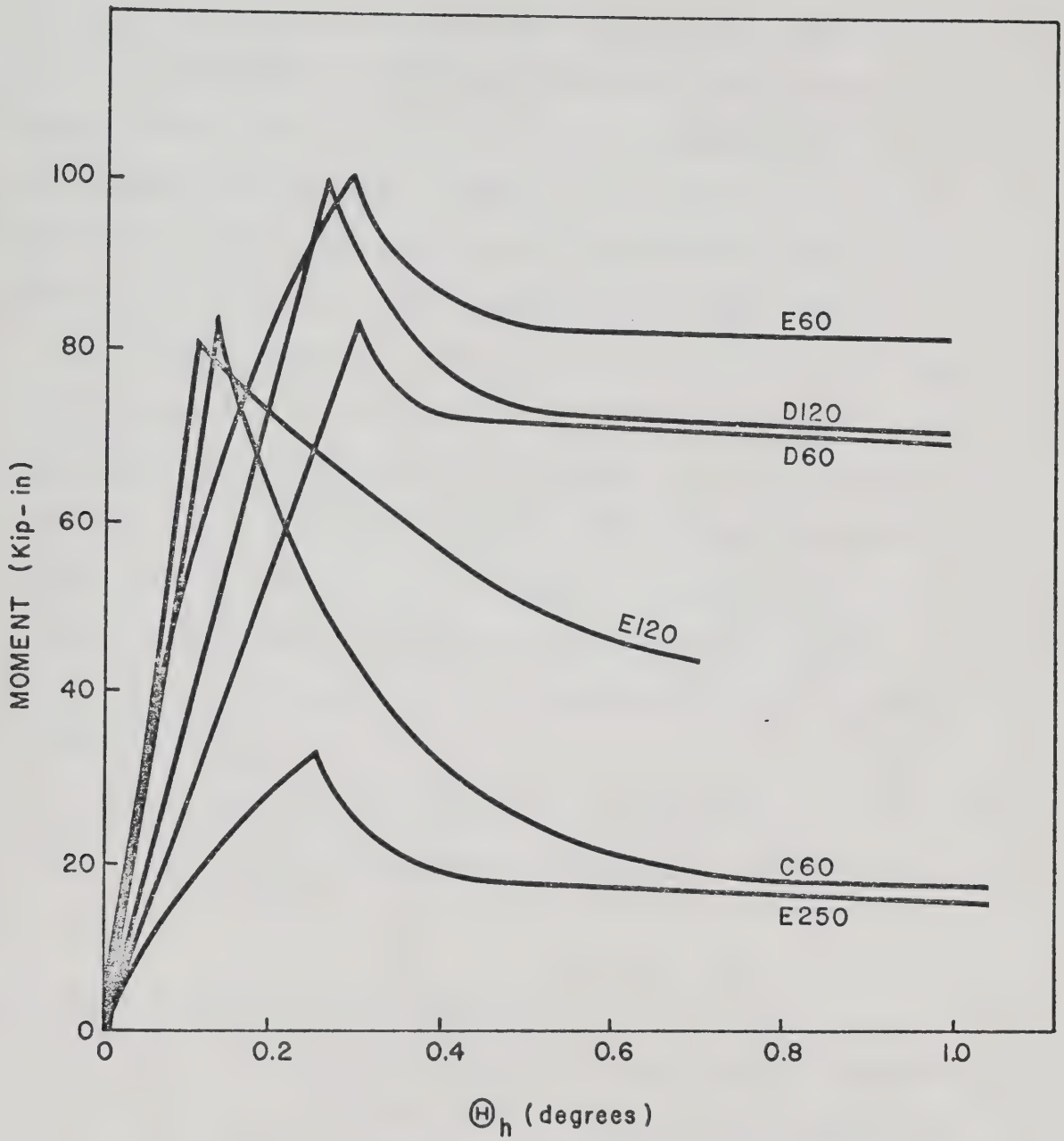

Fig. A.1 Moments vs Slab Rotations For Specimens With Precast Slabs

B. Computer Interaction Diagram

B.1 General

The Fortran program entitled TPM was developed to provide theoretical interaction diagrams for concrete masonry block walls. This program will handle walls of rectangular cross section, with or without reinforcement. Load moment relationships can also be computed for masonry block walls with all cavities grouted or ungrouted.

The main program in TPM relies upon subroutines Prop, Axial, Fsteel, and Inertia to obtain information, balance the loads, calculate the maximum moment for a given load and calculate the equivalent eccentricity of load required to produce such a moment. In analyzing walls with $h/t > 1$. the program calculates the deflection at mid-height using reduced flexural rigidity. The calculated moment includes P-Delta effects.

Output information provided includes the load and moment relationship for maximum stress on a section.

B.2 Basic Assumptions for Analysis

The following basic assumptions were used for analysis:

a. Cross sections which were plane before loading the member remain plane after the load is applied. Accurate measurements have shown that minor deviations from the plane section occur when the load approaches the failure load. However,

theoretical considerations based on this assumption predict test results satisfactorily.

b. The stress-strain relationship for steel is linear until the yield strength of the steel is reached after which it is plastic.

c. Sufficient bonding of the reinforcing bars to the grout is developed to prevent slipping between the two materials. This ensures that the strain in the embedded bar is the same as that of the surrounding grout.

d. The stress-strain relationship of masonry follows a second degree parabola proposed by Hoganstad[14].

e. Since the masonry units or the mortar bond may be cracked, due to shrinkage or other reasons, it is unsafe to take into account their tensile strength.

B.3 Limitations

The following limitations were encountered:

a. The program does not recognize any strength properties given to the section by placing "tie-bars" around the reinforcement.

b. The masonry is considered to have strength only in compression. Any tensile strength is neglected.

c. For reinforced walls the maximum reinforcement should be equal to the balanced reinforcement for flexure.

B.4 Input Data

Fig. B.1 shows the required dimensions and physical properties of the materials to be included in the input data.

The following data refers to a wall reinforced with 3-#6 bars, 121 in. in height. The yield strength of the steel is 60 ksi, the strength of the masonry is 2500 psi and the modulus of elasticity of the steel is 29 X 10^6 psi. The modulus of elasticity of masonry is taken as 1000f'm.

B.5 List of Data

BB = 40 in.	ASC= 0.0 $in.^2$
H = 7.63 in.	FC = 2500 psi
DD = 7.63 in.	FY = 60,000 psi
AS = 1.33 $in.^2$	ES = 29 x 10^6 psi
DC = 3.81 in.	NB = 3
AS(1) = .44 $in.^2$	DS(1) = 3.81 in.
AS(2) = .44 $in.^2$	DS(2) = 3.81 in.
AS(3) = .44 $in.^2$	DS(3) = 3.81 in.
DH = 1.25 in.	HN = 2
WH = 5.13 in	WL = 5.5 in.
RL = 121. in.	

Data File

```
1.  40.,7.63,3.81,3.81,1.33,0.,
2.  2500.,60000.,29000000.,
3.  3,
4.  .44,3.81,
```

```
5.  .44,3.81,
6.  .44,3.81,
7.  1.25,2.,5.13,5.5,121.,
```

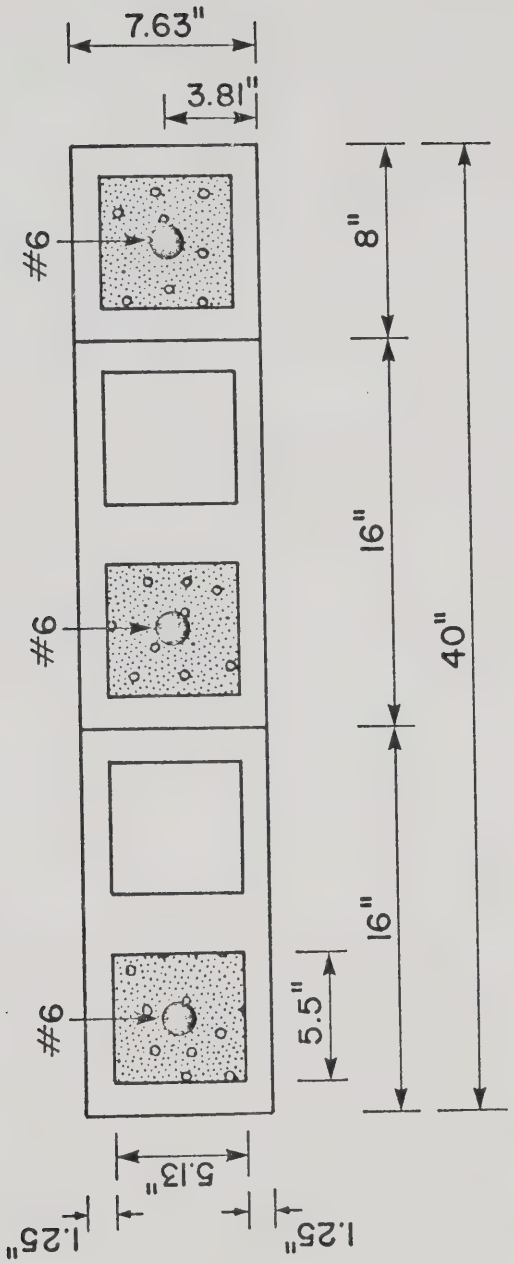

Fig. B.1 Input Data